Analysis of African Easterly Wave Structures and their Role in Influencing Tropical Cyclogenesis

Susanna B. Hopsch, Chris D. Thorncroft and Kevin R. Tyle

Department of Earth and Atmospheric Sciences, University at Albany, State University of New York, Albany, New York

Corresponding author address: Chris D. Thorncroft, Department of Atmospheric and Environmental Sciences, ES-351, University at Albany, State University of New York Albany, NY 12222.

E-mail: chris@atmos.albany.edu

Abstract:

Composite structures of African easterly waves (AEWs) that develop into named tropical cyclones in the Atlantic are compared and contrasted with non-developing AEWs using ECMWF ERA40 reanalysis data and satellite brightness temperature between 1979 and 2001. Developing AEWs are characterized by a more distinctive cold-core structure two days before reaching the West African coast. As they move westwards, the convective activity increases further in the vicinity of the Guinea Highlands region. At the same time the AEW trough increases its vorticity at low-levels consistent with a transformation towards a more warm-core structure before it reaches the ocean. As the AEW moves over the ocean convection is maintained in the trough, consistent with the observed tropical cyclogenesis. The non-developing AEW has a similar evolution before reaching the coast except that the amplitudes are weaker and there is less convective activity in the Guinea Highlands region. The non-developing AEW composite has a more prominent dry signal just ahead of the AEW trough at mid-to-upper-levels. It is argued that the weaker West coast development (i.e. reduced convective activity and reduced spin-up at low-levels) combined with the closer proximity of the trough to mid-to-upper level dry air aloft are consistent with the non-development.

The most intense non-developing AEWs were characterized by more intense convection and stronger mid and low-level synoptic circulations at the West African coast than the developing AEWs. The analysis strongly suggests that the lack of development was due to the presence of dry mid-to-upper-level air just ahead of the

AEW-trough that may have been enhanced due to equatorward advection of dry air by the AEW itself.

1. Introduction

While it is well known that most Atlantic tropical cyclones form in association with synoptic African easterly waves (AEWs, e.g. Avila and Pasch, 1992) our understanding of the processes that influence whether or not one particular AEW will spawn a tropical cyclone is poor. Most previous work on the variability of Atlantic tropical cyclones has emphasized the role of the environment that the AEWs move through, especially the sea surface temperatures (Landsea et al, 1998, Goldenberg et al, 2001; Mann and Emanuel, 2006) and vertical wind shear (e.g. Aiyyer and Thorncroft, 2006). In contrast to these studies the work presented here focuses on the nature of the AEW structures over the West African continent in order to assess the extent to which the AEW structure can increase or decrease the probability of tropical cyclogenesis downstream.

AEWs are synoptic scale systems with a typical wavelength of 2000-4000km. They develop on the African Easterly Jet (AEJ, e.g. Thorncroft and Blackburn, 1999) via a mixed baroclinic-barotropic growth mechanism (e.g. Thorncroft and Hoskins, 1994a) and tend to be triggered by upstream convection (Thorncroft et al, 2008 and refs therein). They usually have peak amplitudes close to the level of the African Easterly Jet (AEJ), around 600 to 700hPa, and at low-levels poleward of the AEJ in the vicinity of the low-level baroclinicity (e.g. Reed et al 1977, Pytharoulis and Thorncroft, 1999). In general, AEWs also possess sub-synoptic scale structures within them. These features are associated with non-linear developments (Thorncroft and Hoskins 1994b), potential vorticity (PV) anomalies generated by convection in mesoscale convective systems (MCSs, e.g. Schubert et al. 1991) or a combination of these. Berry and Thorncroft (2005) suggested that sub-synoptic PV structures travelling with the AEW can often

merge with PV generated by convection in the Guinea Highlands region just before leaving the West African coast. They argued that this can lead to the production of favorable seedlings for downstream tropical cyclogenesis. While this was clearly the case for their AEW the extent to which this is common has not been established.

Hopsch et al. 2007 (henceforth H07) recently investigated the nature and variability of the related vorticity centers at 850hPa, extending the analysis of Thorncroft and Hodges (2001). They confirmed that most of the West African vorticity centers that reach the so-called Main Development Region (MDR, cf Goldenberg and Shapiro, 1996) come from the storm-track that crosses latitudes close to the Guinea Highlands. This is the southern storm track that is located within the peak rainband south of the AEJ (cf Pytharoulis and Thorncroft, 1999). H07 also showed that the numbers of such coherent vorticity centers varies on seasonal, interannual, and decadal timescales. At seasonal and decadal timescales the numbers were significantly and positively correlated with the number of MDR tropical cyclones although, intriguingly, no significant correlation was found at interannual timescales. Despite the interannual result, this analysis suggests that the nature of the AEWs leaving the West African coast may have a role in influencing the probability of downstream tropical cyclogenesis and is a major motivation for this study.

It has long been recognized that African easterly waves (AEWs) are an integral part of the weather and climate over both West Africa and the tropical North Atlantic. The pioneering work of Erickson (1963), Carlson (1969a, b), Simpson et al. (1969), Frank (1970), Burpee (1972) and Reed (1988) introduced the idea that African disturbances could act as seedlings for Atlantic tropical cyclones, a detail that is now

well established (Avila and Pasch 1992; Landsea et al. 1998). These early studies consisted mostly of case studies, including those provided in annual reviews of hurricane activity, or of composite studies using a few AEWs based on data obtained during field experiments, such as GATE (Reed et al. 1977). In previous composite studies of AEWs, the waves have been composited regardless of whether they were later associated with tropical cyclogenesis (see Kiladis et al (2006) and reference therein). This paper provides an investigation of the variability of AEWs and addresses the question of whether the nature and characteristics of the AEWs themselves can influence their fate.

In this paper, the ERA-40 dataset has been analyzed for July-to-September between 1979 through 2001 to generate a climatology of AEW structures leaving the West African coast. By identifying all AEWs that were associated with tropical storms and hurricanes over the MDR, we obtain a composite view of the structure and characteristics of these AEWs. This is compared to the composite of all disturbances/waves that ultimately failed to develop into named tropical cyclones to assess any significant differences in structure and characteristics of these waves.

The layout of this paper is as follows: Section 2 describes the data and method used to diagnose AEWs and the compositing. The structure of the composites of developing and non-developing AEWs is presented and discussed in section 3. The paper is concluded by section 4, offering a brief discussion of the environment and final comments.

2. Methodology

Much of our analysis is based on ECMWF ERA-40 reanalysis data (Uppala, et al. 2005). We chose to restrict our investigation to the period 1979-2001 when satellite data was incorporated into the datastream (e.g. winds and radiances, see Uppala et al, 2005 for more details). The reason for this is that the dataset relies more heavily on the model than observations in the pre-satellite era due to the limited amount of observations in the tropics and over the oceans. The argument can also be made that by restricting the time period to the post-satellite years, all named tropical storms and hurricanes in the tropical Atlantic basin, regardless of their genesis location strength or longevity, should have been detected and thus be accounted for in the best-track dataset of the National Hurricane Center (NHC). It is this latter dataset which provides the time and location for named storms in the MDR.

The AEWs, that form the basis for the composites, are identified by using the streamfunction field at 600hPa derived from 2-6 day filtered winds (based on the 2.5° latitude and longitude grid-resolution). For simplicity, “day 0” for an AEW was defined as the time when a streamfunction minimum was found between 7°N and 20°N at 15°W (approximately the West African coast) and whose magnitude is less than or equal to the mean value for July through September minus one standard deviation. All named storms in the MDR, see Fig. 1, were manually tracked back to West Africa by back-tracking their signature in the vorticity and brightness temperature fields and, whenever possible[1], their associated AEW was identified. These were flagged as “developing AEWs”. The remaining AEWs make up the so called “non-developing AEWs”. This

[1] Two named storms generated their own troughs at the West African coast (i.e. they had no clearly identifiable AEW precursor) and were therefore not included in the composites.

analysis resulted in identification of 512 non-developing AEWs and 91 developing AEWs (see Table 1). Of these 91 developers, 33 became named close to the coast (east of 30°W), 30 in the mid-Atlantic (30°W to 45°W) and 28 in the Western Atlantic (45°W to 60°W). Climatologically speaking, therefore, approximately 1 in 7 AEWs becomes a named tropical cyclone. It should be noted that this ratio varies from month to month. For July, August and September it is approximately 1 in 16, 1 in 4 and 1 in 5 respectively, clearly highlighting an increased "efficiency" between July and the following two months. There is also a notable increase in the number of coastal developments from just 3 in July to 17 in September that is consistent with an increased rainfall and vorticity generation over the Guinea Highlands between those months (c.f. H07).

The high-resolution ERA-40 data (1.125° grid resolution) was used to generate composites of developing and non-developing waves for day-2 to day+2, with day 0 being defined by the trough passage at 15°W, day-2 depicting two days before this and day+2 depicting two days after. It should be pointed out that, while the high-resolution ERA-40 data for all individual members of each composite is used, the composite itself will be relatively smooth due to slight latitudinal and/or longitudinal shift in the fields of the individual sample members, and variations in translation speeds of the systems for the +/-day composites etc. Despite this, comparison between the developing and non-developing AEW composite structures highlights significant differences that will be shown and discussed in the next section.

3. Results

3.1 Horizontal structure of developing AEWs in the east-Atlantic

In this section, we explore the composite horizontal structure of AEWs that were associated with named storms that formed close to the West African coast. This sample consists of all named tropical storms and hurricanes that have their genesis point (defined here as the first point in the NHC best-track dataset) east of 30°W and is clearly the sample that is most likely to be influenced by the nature of the AEWs over the continent.

Figure 2 highlights the AEW structure at 600hPa. For reference here and in subsequent figures we use the 2-6 day filtered streamfunction to depict the large-scale AEW location and structure. At day -2, the AEW trough is weak and located around 10°N close to the Greenwich meridian. The composite of the PV field at 600hPa shows a strip of relatively high PV around 10°N over the continent that extends out over the eastern tropical Atlantic. The high-PV strip spans approximately 5° to 10° of latitude and is accompanied by a PV minimum to the north over the heat low region of the Sahara Desert.

By day -1 the composite AEW trough has deepened and is now more easily seen in the streamfunction field. The trough has moved westward by approximately 10° to near 10°W. The composite trough has also become better defined in the PV field, with a closed PV contour of 0.35 PVU co-located with the streamfunction minimum. The composite trough continues to move westward and is found at 15°W on day 0 (by definition). By this time the streamfunction and PV fields at 600hPa have intensified further. The main PV maximum is found just off the coast of West Africa and, compared to the composite of day -1, the area covered by closed PV contour of 0.35 PVU has

expanded. This is consistent with the generation and merging of diabatically generated PV anomalies in the Guinea Highlands and coastal region (c.f. Berry and Thorncroft, 2005).

Between day+1 and day+2 the composite AEW trough-axis develops a stronger NE-SW tilt, suggestive of a shift towards a more barotropically growing system as the feature moves off shore, (c.f. Kiladis et al (2006)). The intensity of the streamfunction minima weakens slightly when compared to day 0. However, this can be explained by the slightly different translation speeds and tracks of the sampled developing storms. While the large-scale AEW structure (described by the streamfunction) appears somewhat weaker at these later times, interestingly the PV field at 600hPa maintains its strength and actually expands in size as the AEW moves off shore. This is consistent with the fact that by day+2, 29 of the 33 tropical cyclones that form close to the coast have reached or passed their first point in the NHC best track dataset.

Figures 2f through j show the evolution for day -2 to day +2 for the non-developing AEWs. The non-developing composite AEW trough is weaker throughout the selected time period. This is highlighted by both the streamfunction, which is about 50% weaker, and the PV, which is about 33% weaker. In addition to being weaker, the PV maximum in the non-developing AEW shifts into the south-westerlies as it moves over the ocean. This is somewhat consistent with a shift of the peak convection from the trough to the south-westerlies noted in the composite study of Kiladis et al (2006) (see also Fig. 4 below).

From Thorncroft and Hodges (2001) and H07 we know that low-level relative vorticity can be used to obtain an appreciation of sub-synoptic scale characteristics of

AEWs. Figure 3 shows the evolution from day -2 to day +2 of the composite relative vorticity at 850hPa for the developing and non-developing AEWs. The southern storm track for the developing AEW along 10°N is generally more active than the northern track for all days. The 850hPa relative vorticity composite for day -1 shows a local maximum at the leading edge of the composite AEW trough (over the Guinea Highlands region), consistent with convection that is located in the northeasterlies at this time. As the AEW trough passes over 15°W on day 0, this relative vorticity feature intensifies, obtains a more circular shape and is in the center of the large-scale AEW trough. This suggests a strong coupling between the AEWs and convection (and is confirmed by composites using Brightness Temperature, see below). As the system moves off shore (Figs. 3 d, e), the main region of high relative vorticity within the AEW shifts towards the trailing edge of the trough and is found in the south-southwesterlies. This is somewhat consistent with KTH06, who found that convection shifts into the southerly flow as the waves propagate into the Atlantic.

The evolution of the non-developing AEWs is shown for comparison in Figs.(3 f, j). In contrast to the developing AEW, the northern and the southern storm tracks have similar relative vorticity values. As the non-developing AEW approaches the West African coast, the magnitudes and intensification rate in the southern storm track are weaker than those for the developing AEW composite. The relative vorticity values increase from about 2.0 x 10^{-5} s^{-1} to only 3.0 x 10^{-5} s^{-1} compared to the increase from about 3.0 x 10^{-5} s^{-1} to about 4.5 x 10^{-5} s^{-1} in the developing composite. The vorticity centre also becomes much less distinct and shifts to the east of the mid-level trough as the system moves off shore.

Figure 4 presents the composites of brightness temperature from the Cloud Archive User Service (CLAUS) dataset (see Hodges et al, 2000) and 600hPa streamfunction for the developing and non-developing AEWs. Consistent with KTH06 and the aforementioned relative vorticity signatures the most active convection is found in north-northeasterlies over land (at 600hPa), moves to the center of the trough as the system approaches the West African coast, where convective activity is strongly enhanced, and finally shifts into the south-southwesterly flow when the AEW is over the tropical Atlantic Ocean. The convective signature of the non-developing AEW is less pronounced throughout the five-day period. There is a slight increase in convection as the AEW approaches the coast between day -1 and day 0 (Figs. 4 g and h) but it is clearly not as convectively active (with a minima of about 255K compared to about 240K).

In summary, the horizontal structures presented above clearly indicate that the developing AEWs have more intense troughs, both in terms of their mid-level PV and related streamfunction minimum, when compared to non-developing AEWs. They are also characterized by more intense low-level vorticity centers in the southern storm track and, consistent with this, are more convectively active. These composites suggest that AEWs that are more convectively active in the Guinea Highlands region provide more favorable “seedlings” for tropical cyclogenesis, consistent with the hypothesis of Berry and Thorncroft (2005). We now consider the differences in vertical structure.

3.2 Vertical structure of developing AEWs in the east Atlantic

Further insight into the differences between developing and non-developing AEWs can be gained by considering the evolution of their vertical structures (Fig. 5). At day-2 the mid-level troughs of both the developing and non-developing AEWs are located near the Greenwich meridian (c.f. Fig. 2). The developing AEW is characterized by peak relative vorticity values around 700 - 600hPa that are notably larger than those for the non-developing composite (c.f. Figs. 5(a,b)). Regions of enhanced upward vertical motion are present at the West African coast, consistent with enhanced convective activity in the Guinea Highlands region.

By day 0, the peak relative vorticity in the trough of both AEWs has increased (Figs. 5c and d), consistent with growing AEWs and figures shown earlier. In the developing AEW the vorticity maximum has lowered to around 850hPa consistent with a developing warm-core structure. In contrast, the relative vorticity of the non-developing AEW composite increases less markedly. Consistent with the differences in relative vorticity, and the convective activity (Fig. 4) the peak ascent is about 30% stronger in the developing AEW.

The cross-sections highlight the presence of moist low-level layers over land and the ocean in both the developing and non-developing AEWs. However, the largest differences in relative humidity occur in the mid-to-upper levels close to and just downstream of the AEW troughs. For the developing AEW, the trough is characterized by relative humidity values in excess of 80% throughout a deep layer (up to around 300hPa). For the non-developing AEW, such large humidity values only extend to

around 500hPa in the trough, clearly consistent with the observed weaker convective activity. A second striking difference can be seen at mid-to- upper levels downstream of the AEW troughs where relative humidity is noticeably lower for the non-developing case. Note for example the larger region of air with relative humidities less than 50%. This suggests that the proximity of the AEW trough to dry air could be an influencing factor for tropical cyclogenesis. Dunion and Velden (2004) have suggested a negative role for the Saharan air layer (SAL) over the Atlantic. In contrast, the biggest dry signal here is above the SAL in the mid-to-upper troposphere. The possible negative role of dry air in the upper-troposphere on tropical cyclogenesis has also been noted recently by Braun (2009).

After an additional two days the AEW troughs have moved over the ocean to approximately 30°W. The developing AEW has maintained a relative vorticity maximum at low levels (Fig.5(e) top). It is accompanied by a deep moist layer with relative humidities greater than 70% and ascent exceeding -18Pas^{-1} (Fig. 5e bottom). In contrast, the non-developing AEW weakened and has no discernable relative vorticity maximum (Fig.5f). In the vicinity of the weak trough vertical velocities are very weak (around -0.03Pas^{-1}), and the air above 600hPa is very dry, consistent with weak or no deep convection. The only region with distinctive upward vertical velocities in the non-developing AEW composite cross section is at the West African coast and Guinea Highlands region.

The composite results strongly suggest that the typical structure of developing AEWs is different from that of non-developing AEWs. The developing AEWs are convectively more active at the West African coast and Guinea Highlands region and,

consistent with this, have stronger mid-level PV and low-level vorticity. The developing AEWs appear to develop a stronger warm core structure as the system approaches the West African coast, manifested in the lowering in the level of the relative vorticity maximum to around 850-925hPa. In comparison, the non-developing AEWs are weaker and are also clearly associated with drier mid-to-upper-level air just downstream of the AEW trough.

3.3 Variability

The composite maps and cross sections that were described above provide a smoothed signature of the most common features in the individual sample members. The smooth appearance is due to slight differences in structure, location of the AEW troughs and minor latitudinal and/or longitudinal shifts in the fields of the sampled waves. The smoothing effect should be particularly enhanced in the non-developing AEW composites, since its sample size is more than fifteen times larger than that for the developing AEW composite. It is important to know the spread of quantities such as PV and relative vorticity within the two composite groups. This is achieved by considering the peak PV and relative vorticity values of all of the AEWs between day-2 and day-0. The sampled trough locations for the three days was taken along 8°-16°N, and 5°W-5°E for day -2, 15°W-5°W for day -1 and 20°W-10°W for day 0.The data was then binned and the relative percentage of the sample members within each bin was calculated.

Figure 6 shows the resulting histograms of PV at 600hPa for the developing and non-developing AEWs. The figure shows that the average PV increases slightly as the AEWs move westward and that there is a tendency towards higher values of PV at

600hPa for the developing AEWs for days -2, day -1 and day 0. A simple t-test with the null-hypothesis that the two distributions at day 0 (developing and non-developing) are the same was rejected and the difference between the two distributions is statistically significant at the 99% confidence level.

Figure 7 shows histograms, using the same approach, for the vertical difference of relative vorticity between 850hPa and 600hPa. The figure shows that most developing systems have stronger mid-tropospheric relative vorticity than the non-developing systems at day-2. In contrast, the distribution for the non-developing AEWs shows no preference for stronger relative vorticity at 600hPa or 850hPa. By day-1 the distribution of the difference of relative vorticity between the two layers for developing and non-developing AEWs is nearly identical (differences are statistically insignificant). By day 0, however, the two distributions again show distinctive – and statistically significant – differences, with the developing AEWs now showing a large fraction of systems with larger relative vorticity at 850hPa than at 600hPa, and the non-developing AEWs showing only small differences between relative vorticity at the two levels.

These results point to interesting differences in the structure of the developing and non-developing AEWs. Developing AEWs have a more pronounced cold-core structure at day -2 inland and a more warm-core structure at day 0 at the coast. The more pronounced cold core structure at day-2 is consistent with a more intense AEW but also one that is more convectively active (see Fig. 4). For example, we would expect enhanced MCS activity in the vicinity of the trough, and associated stratiform convection in particular, to be associated with more mid-level PV and a more intense cold core trough (c.f. Berry and Thorncroft, 2005). The stronger cold core troughs and related low

convective inhibition might subsequently be more favorable to deep convection in the Guinea Highlands than the weaker non-developing AEWs, and this convection likely influences the cold-core to warm-core transition. The precise details of this transition need to be explored in more detail.

From the histograms it is clear that there are numerous intense systems in the non-developing AEW group that have high values of PV at 600hPa. Since one would expect these more intense systems to be associated with successful storm formation downstream rather than with dissipating systems, we now examine these a little more closely. For that purpose, the 33 most intense (I33) non-developing AEWs for PV at 600hPa were selected for a supplementary composite study.

Figure 8 shows the composite results for both developing AEWs (left hand side, repeated here for ease of comparison) and the I33 AEWs (right hand side) for day -2, day 0 and day +2. The I33 AEW-trough is much stronger than the developing AEW-trough at day -2 and at day 0. At both times it is characterized by stronger PV values. While the positive PV anomaly associated with the I33 AEW trough at day 0 is notably more intense than for the developing case, it is also clear that lower values of PV (around 0.1PVU) are being advected equatorwards at the leading edge of the trough. Given that the likely source of this low-PV air is the Sahara, this is highly suggestive of the fact that the Saharan air layer (SAL) is having a more significant role in the evolution of the I33 AEW trough than for the developing AEW trough. As we will discuss below, this may have had a negative impact on the development of the I33 AEW trough. As the I33 AEW-trough moves off the West African coast (Fig. 8f) the PV anomaly decreases and is comparable to the developing AEW-trough by day+2. The rapid decrease in PV

might have been contributed to by the continued advection of lower PV air, and lateral mixing at the leading edge of the I33 AEW-trough. Also, at day+2 the maximum PV values are found to the east of the composite AEW trough. The developing AEW composite, in contrast, maintains the PV maximum within the trough axis of the translating system.

Figure 9 shows vertical cross sections for the I33 AEW composite for day -2, day 0 and day +2. The cross section is taken along the same latitude and longitude band as the cross sections shown earlier in section 3.2. The I33 AEW-trough at day -2 is found just east of the Greenwich meridian and is associated with a distinctive mid-level relative vorticity maximum, consistent with the fact that the 33 strongest non-developing AEWs were used. The strongest vertical motion is found close to the AEW trough and also in the region of the Guinea Highlands at the West African coast. The relative vorticity increases as the composite AEW reaches the West African coast on day 0. Although the I33 AEW-trough intensifies as it moves towards the coast, the relative vorticity increases throughout the column below about 500hPa resulting in a relatively uniform distribution between 600hPa and 850hPa (in fact, the I33 AEW remains cold core throughout the composited day range, not shown). Also, consistent with the low-PV seen ahead of the I33 AEW-trough in Fig. 8, the relative humidity of the air just ahead of the trough at mid-to-upper levels (between about 700hPa and 200hPa) is lower than that of the developing AEW with a much larger region of air with relative humidities less than 50%. By day +2 the I33 AEW-trough's relative vorticity has decreased, and is no longer aligned with the composite trough. The strongest vertical velocities are no longer associated with this AEW, but (as for the composite of all non-developers) are found

over the Guinea Highlands region. The mid-to-upper level air close to and just ahead of the I33 AEW-trough continues to be much drier than in the developing AEW case.

The comparison of the I33 AEW composite and the developing AEW composite raises some interesting issues. The I33 AEW trough at day 0 is characterized by a strong positive PV anomaly at 600hPa and an associated column of high relative vorticity at the coast. From a dynamical perspective this would seem like a more ideal "seedling" than the developing AEW composite. The first hint of the likely hindrance to the development of this seedling was noted in the PV distribution just ahead of the I33 AEW trough where anomalously low-PV air was being advected southwards ahead of it at 600hPa. The vertical cross-sections highlighted the fact that this air is relatively dry, consistent with a Saharan or high altitude origin. We hypothesize that the close proximity of the I33 AEW-trough to the dry air is the reason for the lack of development. Again, this is somewhat consistent with the ideas of Dunion and Velden (2004) who have associated a reduction or delay in tropical cyclone intensification to the presence of the Saharan Air Layer. In the present case it should be noted, however, that the dry layer observed ahead of the I33 AEW-trough extends higher into the troposphere than the SAL suggesting that air above the SAL (which is also likely to be dry) could be having a role.

One inference from the discussion above would appear to be that it is possible that AEWs can be too strong to develop into tropical cyclones. A stronger AEW will advect dry air equatorwards ahead of the trough at a faster rate than a weak AEW. If this dry air is entrained into the convecting region within or close to the AEW trough it will hinder any developments in the vicinity of the AEW-trough. This is a somewhat

surprising conclusion and deserves more scrutiny in future work. Indeed this suppression can be seen in the composite of the I33 AEW with brightness temperature (Fig. 10). While at day-0 the convection is more intense than for the developing AEW composite there is a more pronounced suppression to the convection in the region of north-easterlies just ahead of the trough (c.f. Figs. 4 and 10). The convective activity in the vicinity of the I33 AEW trough weakens during the next two days suggesting the possible negative impact of the dry air ahead of and in the vicinity of the trough.

3.4 Comparison with AEWs associated with tropical cyclogenesis in the mid and western Atlantic

The analysis above has highlighted the significant differences between AEWs that do not develop and those that develop close to West Africa (15°W-30°W). The difference is related to the dynamic and thermodynamic processes that take place over the West African coastal and Guinea Highlands regions. Given that these coastal developments account for roughly one third of the total number of AEW-developments in the MDR and given that we might expect the nature of the AEWs leaving West Africa to become less influential further away, we briefly consider whether there are similar significant structural differences associated with AEWs that develop in the mid-Atlantic (30°W-45°W) and western Atlantic (45°W-60°W) (see Fig. 1). As indicated in Table 1, these two additional areas include 30 and 28 additional named tropical cyclones respecitively, accounting for nearly two thirds of all MDR tropical cyclones.

Figure 11 (a,b,c) shows the composite day-0 structure of the AEWs that were associated with tropical cyclones in the mid- Atlantic region. The dynamical structure of the AEWs that develop into named storms in the Mid-Atlantic (Fig. 11(a,b)) has a similar structure but weaker amplitude than the coastal developing AEWs (Fig. 2, 3). In this sense their character falls somewhere between the developing coastal AEWs and non-developing AEWs. This strongly suggests that the nature of AEWs leaving the West African coast can have a role in influencing the probability of tropical cyclogenesis in the mid-Atlantic, although the "memory" of that structure is clearly poorer than for coastal developments.

Further evidence of this is indicated in the composite brightness temperature field (Fig. 11(c)) which highlights the presence of enhanced convection over the Guinea Highlands (compared to non-developers). What is also notable about the convection at day-0 of this composite is the lack of suppressed signal in the convection in the north-west quadrant of the AEW-trough. As discussed previously, this suggests a weakened impact of mid-level dry advection compared with the non-developers. West-east vertical cross-sections of the relative humidity (not shown) are consistent with this.

For completeness the composite of the day-0 AEWs that were associated with tropical cyclogenesis in the Western Atlantic is included in Fig. 11(d,e,f). The structure is very similar to that obtained for the mid-Atlantic, albeit a little weaker. This suggests that, even for the cases of tropical cyclogenesis in the West Atlantic, the nature of the AEWs leaving the West African coast is important to consider and is significantly different from AEWs that did not develop (c.f. Fig. 2, 3). Thus, despite the fact that it takes approximately 3-4 days for AEWs to reach the West Atlantic, the nature of the

AEWs leaving the West African coast still appears to have an influence on tropical cyclogenesis there. Put simply, tropical cyclogenesis in the whole of the MDR is most likely to be associated with AEWs leaving the West African coast that are dynamically strong (in terms of its mid and low-level circulations) and convectively active.

4. DIscussion and final comments

All AEWs that were associated with tropical storms and hurricanes over the main development region (MDR) were identified between July and September, and for the years 1979 – 2001. The data was used to obtain a composite view of the structure and characteristics of these AEWs and their large-scale environment. This was compared to the composite of all AEWs that ultimately failed to develop into named tropical cyclones. Substantial and significant differences exist between the structures of developing and non-developing AEWs.

The developing AEW composite is characterized by a distinctive cold-core structure at day-2, when its trough is located close to the Greenwich meridian. This is consistent with a stronger AEW-trough and more intense MCS activity embedded within it (c.f. Berry and Thorncroft, 2005). As the developing AEW moves towards the West African coast, the convective activity increases further in the vicinity of the Guinea Highlands region. At the same time low-level vorticity in the AEW trough increases consistent with a transformation towards a warm-core structure. As the AEW moves over the ocean convection is maintained in the trough, consistent with the observed tropical cyclogenesis.

The non-developing AEW has a similar evolution between day-2 and day-0 except that the amplitudes are weaker and there is less convective activity in the Guinea Highlands region. Consistent with this are weaker low-level circulations and an AEW that continues to be characterized by a cold-core structure. What is also striking about the non-developing AEW composite is a more prominent dry signal just ahead of the AEW trough at mid-to-upper-levels. From this we suggest that the weaker West coast developments (i.e. reduced convective activity and reduced spin-up at low-levels) combined with the closer proximity of the trough to mid-to-upper level dry air aloft are consistent with the non-development.

Further insight was gained by considering the most intense AEWs (defined by the PV at 600hPa) that did not develop. These AEWs were associated with more intense convection at the West African coast than the developing AEWs and, consistent with this, were characterized by higher vorticity throughout the mid-to-lower troposphere. Although these appear to be ideal seedlings for tropical cyclogenesis they did not develop. Instead, as these AEWs move over the ocean, the convection weakens and shifts into the south-westerlies consistent with previous climatological studies that considered all AEWs (cf KTH06). We hypothesize that the weakening convection and lack of tropical cyclogenesis is due to the presence of dry mid-to-upper-level air just ahead of the AEW-trough, consistent with the composite of all non-developers. We argue that this dry air arises in association with the strong equatorward advection of dry air by the AEW itself. This would suggest that some AEWs might be too strong to develop and that, in some sense, each AEW may possess the seeds of their own destruction. This clearly requires closer scrutiny including examination of individual

events. Also, in contrast to Dunion and Velden (2004), these composites highlight the potential negative impact of dry air above the SAL which may have originated from higher latitudes and altitudes (c.f. Braun, 2009 and Roca et al 2005).

The previous sections presented an overview of the differences in structure for developing and non-developing AEW composites. Another aspect that has not been addressed so far is the contribution or possible impact of the large scale environment on the development of these waves. The question addressed here is whether the differences in the composite AEW structure are sufficient to explain the differences in the AEWs' outcome, or whether it is the character of the large-scale environment through which the AEWs move that is the determining factor for development, or whether it is a combination of both.

Here we briefly consider two large-scale environmental factors known to be important for genesis and intensification of tropical cyclones: vertical wind shear (taken over a layer between 200-850hPa) and SSTs. Tropical cyclogenesis tends to be favored by low wind shear (e.g. Goldenberg and Shapiro, 1996), and high SSTs (e.g. Landsea et al 1998). A complication that arises with regards to the wind shear for the individual days of the AEW composites is that the shear of the systems themselves is part of the resulting composite. However, the goal here is to examine the role of the environmental tropospheric deep wind shear. This problem can be minimized in part by instead considering the average of the composite five-day period, since the individual systems' impact on the large-scale shear is largely, but not entirely, reduced in the resulting average. The SST composites are less problematic since, given the relatively weak low-

level winds in AEWs, the SSTs during the 5-days of the compositing are likely not impacted by the AEWs themselves.

Figure 12 shows the five-day average of the mean 200-850hPa wind shear for the developing, and non-developing AEWs and their difference. The spatial structures of the composite shear for the two composites over West Africa and the tropical North Atlantic are both very similar to climatology (c.f. Fig.3 in Aiyyer and Thorncroft 2006) with highest shear linked to the tropical easterly jet in the West African region and the sub-tropical westerly jet in the sub-tropical Atlantic. The difference between the tropospheric deep wind shear between developing and non-developing AEWs in the immediate genesis region for coast storms (i.e. first point of named storms in the best-track dataset occurs east of 30°W) is very small (Fig. 12(c)) suggesting that tropospheric deep wind shear plays a small role in determining the fate of these AEWs. We should note however that there is enhanced shear in the southern part of the MDR with peak anomalies around 10^{o}N. This is associated with a stronger tropical easterly jet (c.f. Figs 12(a,b)) that itself is consistent with a wetter West African continent (Newell and Kidson, 1984). This is consistent with the convectively active AEWs contributing to this composite.

Figure 13 shows the composites using the weekly SST data set and shows that warm SSTs, with temperatures above 26°C (sufficient to support tropospheric deep convection), are present within the MDR for both the developing (Fig. 13(a)) and non-developing (Fig.13(b)) AEWs. The difference between these two composites, Fig. 13(c), shows that SSTs in the immediate proximity of the West African coast (around 20°N, where the background SST gradient is strongest) are up to 1°C warmer in the

developing composite. While most tropical cyclones form well to the south of this warm anomaly (see Fig. 1), it is possible that air inflowing into the developing tropical cyclone could have a trajectory that passes over this water. Thus, the possibility that this warm SST anomaly can favor tropical cyclogenesis cannot be ruled out and should be investigated in the future.

In conclusion, the results presented in this paper strongly suggest that the nature of the AEWs leaving the West African coast can impact the probability of tropical cyclogenesis in the Eastern Atlantic. Consistent with the hypothesis originally proposed by Berry and Thorncroft (2005) AEWs that are convectively active in the vicinity of the Guinea Highlands can intensify and develop strong low-level circulations in the vicinity of the trough making them ideal seedlings for tropical cyclogenesis. More detailed analysis of these convective developments is required, combining observations and high resolution modeling. The relative roles played by PV anomalies moving westwards with the AEWs, and those that develop in situ should be explored. Another major area of future research is to unravel the source and impact of the mid-to-upper-level dry air associated with the non-developers. Considerable insight might be gained by looking at case studies of the most intense non-developers in particular. In addition to the nature of the AEW, the probability of tropical cyclogenesis is of course influenced by the environment through which the AEWs propagate. Unraveling the relative roles of the AEW seedlings and the environment remains a difficult area but needs to be studied through more analysis of observations and modeling.

Acknowledgments: This research was supported by the National Science Foundation under Grant ATM-0507976. CLAUS data are available at the British Atmospheric Data Centre (BADC; http://badc.nerc.ac.uk/cgi-bin/data_browser/data_browser/badc/claus/).

References

Aiyyer, A.R., and C. Thorncroft, 2006: Climatology of Vertical Wind Shear over the Tropical Atlantic. J.Climate, 19, 2969–2983.

Avila L., and R. J. Pasch, 1992: Atlantic tropical systems of 1991. Mon. Wea. Rev., 120, 2688–2696.

Berry, G., and Thorncroft, C. 2005: Case study of an intense African easterly wave. Mon. Wea. Rev., 133, 752-766.

Braun, S. A. 2009: A climatological perspective of the role of the Saharan Air Layer in Atlantic tropical cyclogenesis and evolution. Mon. Wea. Rev., submitted.

Burpee R. W., 1972: The origin and structure of easterly waves in the lower troposphere of North Africa.J. Atmos. Sci., 29, 77–90

Carlson, T.N., 1969a: Synoptic Histories of Three African Disturbances that Developed into Atlantic Hurricanes. Mon. Wea. Rev., 97, 256–276.

Carlson, T.N., 1969b: Some Remarks on African Disturbances and Their Progress over the Tropical Atlantic. Mon. Wea. Rev., 97, 716–726

Dunion, J. P., and C. S. Velden, 2004: The impact of the Saharan air layer on Atlantic tropical cyclone activity. Bull. Am. Meteor. Soc., 85, 353-365.

Emanuel, K., 2003: Tropical Cyclones. Ann Rev. Earth Planet. Sci., 31, 75-104.

Erickson, C.O., 1963: An Incipient Hurricane near the West African Coast. Mon. Wea.

Rev., 91, 61–68.

Frank, N. L., 1970: Atlantic Tropical Systems of 1969. Mon. Wea. Rev., 98, 307-314.

Goldenberg, S.B., and L.J. Shapiro, 1996: Physical Mechanisms for the Association of El Niño and West African Rainfall with Atlantic Major Hurricane Activity. J. Climate, 9, 1169–1187.

Goldenberg S., C. W. Landsea, A. M. Mestas-Nuñez, and W. M. Gray, 2001: The recent increase in Atlantic hurricane activity: Causes and implications. Science, 293, 474–479.

Hall, N.M.J., G.N. Kiladis, and C.D. Thorncroft, 2006: Three-Dimensional Structure and Dynamics of African Easterly Waves. Part II: Dynamical Modes. J. Atmos. Sci., 63, 2231–2245.

Hodges, K. I., D. W. Chappel, G.J. Robinson and G. Yang, 2000: An improved algorithm for generating global window brightness temperatures from multiple satellite infrared imagery. J. Atmos. Oceanic Technol., 17, 1296-1312.

Hopsch, S.B., C.D. Thorncroft, K. Hodges, and A. Aiyyer, 2007: W est African Storm Tracks and Their Relationship to Atlantic Tropical Cyclones. J. Climate, 20, 2468–2483.

Kiladis, G.N., C.D. Thorncroft, and N.M.J. Hall, 2006: Three-Dimensional Structure and Dynamics of African Easterly Waves. Part I: Observations. J. Atmos. Sci., 63, 2212–2230.

Landsea C., G. D. Bell, W. Gray, and S. B. Goldenberg, 1998: The extremely active 1995 Atlantic hurricane season: Environmental conditions and verification of

seasonal forecasts. Mon. Wea. Rev., 126,1174–1193.

Mann, M. E., and K. A. Emanuel, 2006: Atlantic hurricane trends linked to climate change. EOS, 87, 233-244.

Newell, R.E. and J.W. Kidson, 1984: African mean wind changes between Sahelian wet and dry periods, J. Climatol., 4, 27-33.

Pytharoulis, I. and Thorncroft, C.D. 1999: The low-level structure of African easterly waves in 1995. Mon. Wea. Rev., 127, 2266-2280.

Reed, R.J., D.C. Norquist, and E.E. Recker, 1977: The Structure and Properties of African Wave Disturbances as Observed During Phase III of GATE. Mon. Wea. Rev., 105, 317–333.

Reed, R. J., 1988: On understanding the meteorological causes of Sahelian drought. Persistent Meteo-Oceanographic Anomalie and Teleconnections, C. Chagas and G. Puppi, Eds., Pontificae Academiae Scientiarvm, 179–213.

Roca,R., J.-P. Lafore, Piriou, C., and Redelsperger, J.-L. 2005: Extratropical dry intrusions into the West African Monsoon Midtroposphere: An important Factor for the Convective Activity over the Sahel, J. Atmos. Sci., 62, 390-407

Schubert W.H., P.E. Ciesielski, D.E. Stevens, and H.-C. Kuo, 1991: Potential vorticity modeling of theITCZ and the Hadley circulation. J. Atmos. Sci., 48, 1493–1500.

Simpson R. H., N. Frank, D. Shideler, and H. M. Johnson, 1969: Atlantic tropical disturbances of 1968.Mon. Wea. Rev., 97, 240–255.

Thorncroft, C.D. and Hoskins, B.J. 1994a: An idealized study of African easterly waves. I: A linear view. Q.J.R. Meteorol. Soc., 120, 953-982.

Thorncroft C., and B. J. Hoskins, 1994b: An idealized study of African Easterly Waves,

Part II: A nonlinear view. Quart. J. Roy. Meteor. Soc., 120, 983–1015.

Thorncroft, C., and K. Hodges, 2001: African Easterly Wave Variability and Its Relationship to AtlanticTropical Cyclone Activity. J. Climate, 14, 1166–1179.

Thorncroft, C.D., N.M.J. Hall, and G.N. Kiladis, 2008: Three-Dimensional Structure and Dynamics of African Easterly Waves, Part III: Genesis. JAS, in press.

Uppala S. M., Coauthors, 2005: The ERA-40 re-analysis. Quart. J. Roy. Meteor. Soc., 131, 2961–3012.

Table 1: Number of developing and non-developing AEWs per month (top two rows); and the number of named tropical cyclones associated with AEWS according to where they were first named (bottom three rows). East Atlantic is represented by the box between 7°N-20°N and 30°W-15°W. Mid-Atlantic is represented by the box between 7°N-20°N and 45°W-30°W. West Atlantic is represented by the box between 7°N-20°N and 60°W-45°W.

FIGURE CAPTIONS

FIGURE. 1. Genesis points of all named storms in the MDR from the NHC best track data set for July-September 1979-2001. The boxes form the boundaries from which the Eastern Atlantic, Central Atlantic and Western Atlantic composites were constructed.

FIGURE. 2. Composites of developing (left) and non-developing (right) AEWs for the five-day period centered on the day of trough passage at 15°W. Fields shown are 600 hPa streamfunction (solid and dashed lines, based on 2-6 day filtered winds) and 600 hPa potential vorticity (PVU, shaded).

FIGURE. 3. Composites of developing (left) and non-developing (right) AEWs for the five-day period centered on the day of trough passage at 15°W. Fields shown are 600 hPa streamfunction (solid and dashed lines, based on 2-6 day filtered winds) and 850 hPa relative vorticity ($10^{5}s^{-1}$, positive values only, shaded).

FIGURE. 4. Composites of developing (left) and non-developing (right) AEWs for the five-day period centered on the day of trough passage at 15°W. Fields shown are 600 hPa streamfunction (solid and dashed lines, based on 2-6 day filtered winds) and brightness temperature (shaded).

FIGURE. 5. Cross-sections of the AEW composites for days -2, 0, and +2; developers (non-developers) are displayed in figs. 5a, 5c, and 5e (5b, 5d, 5f). The cross-sections fall along 11.25°N between 40°W and 10°E in the horizontal, and from 1000 hPa to 100 hPa in the vertical. The top half of each figure displays relative vorticity (10^{-5} s^{-1}, shaded), equivalent potential temperature (degrees K, black contours), and horizontal wind barbs (knots). The bottom half shows relative humidity (%, shaded) and vertical velocity (hPa s^{-1}, black contours). The approximate location of the composite AEW trough is indicated by the red diamond.

FIGURE. 6. Histograms of PV (PVU) at 600hPa for the developing (light gray bars) and non-developing AEWs (dark gray bars) for (a) day -2 (b) day -1 and (c) day 0. The sampled trough locations for the three days covered an 8°x10° lat-lon box with bounds 8°-16°N (all three days), 5°W-5°E for day -2, 15°W-5°W for day -1 and 20°W-10°W for day 0.

FIGURE. 7. As in Fig. 6. but for the difference in relative vorticity (10^{-5} s^{-1}) between 850 and 600 hPa for (a) day -2, (b) day -1 and (c) day 0. Positive (negative) values of the difference denote greater (less) vorticity at 850 hPa than at 600 hPa.

FIGURE. 8. Composites of developing (left) and the 33 most intense non-developing (right) AEWs for days -2, 0, and +2. Fields shown are 600 hPa streamfunction (solid and dashed lines, based on 2-6 day filtered winds) and 600 hPa potential vorticity (shaded).

FIGURE. 9. As in Fig. 5 a-c, but for the 33 most intense non-developing AEWs.

FIGURE. 10. 600 hPa streamfunction (contour lines) and CLAUS brightness temperature for the 33 most intense non-developing AEWs.

FIGURE. 11. Day 0 600 hPa streamfunction, overlaid with (a) 600 hPa potential vorticity (PVU, shaded); (b) 600 hPa relative vorticity ($10^{-5}$$s^{-1}$, shaded); (c) CLAUS brightness temperature (K, shaded) for developers in the mid-Atlantic region of the MDR; (d-f) are as in (a-c), but for the western Atlantic.

FIGURE. 12. Day -2 to day +2 average of composite wind shear (m s^{-1}) between 200 and 850 hPa of (a) developing and (b) non-developing AEWs and (c) the difference between (a) and (b). The position of the composite 850 hPa relative vorticity maximum is shown by the green diamond in (a) and (b).

FIGURE. 13. Composite of weekly SST (K) for (a) developers and (b) non-developers, with (c) the difference between (a) and (b). The position of the composite 850 hPa relative vorticity maximum is shown by the yellow diamond in (a) and (b).

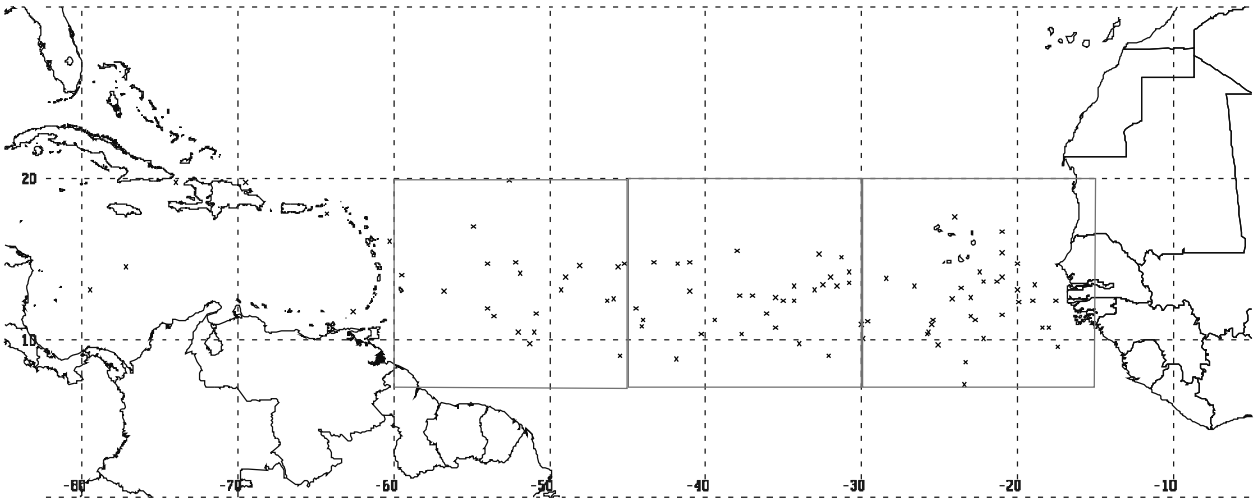

FIG. 1. Genesis points of all named storms in the MDR from the NHC best track data set for July-September 1979-2001. The boxes form the boundaries from which the Eastern, Central and Western Atlantic composites were constructed.

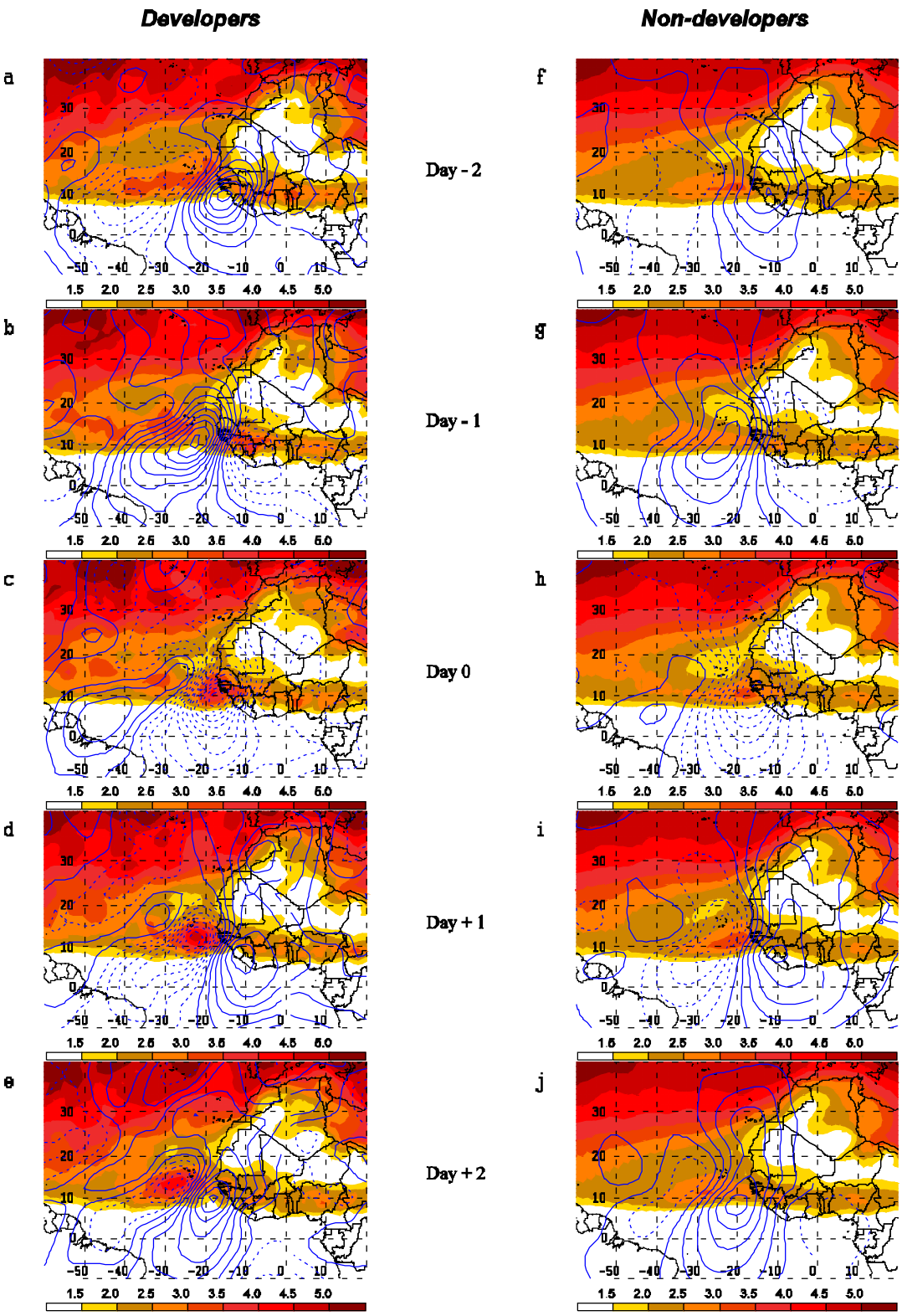

FIG. 2. Composites of developing (left) and non-developing (right) AEWs for the five-day period centered on the day of trough passage at 15°W. Fields shown are 600 hPa streamfunction (solid and dashed lines, based on 2-6 day filtered winds) and 600 hPa potential vorticity (PVU, shaded).

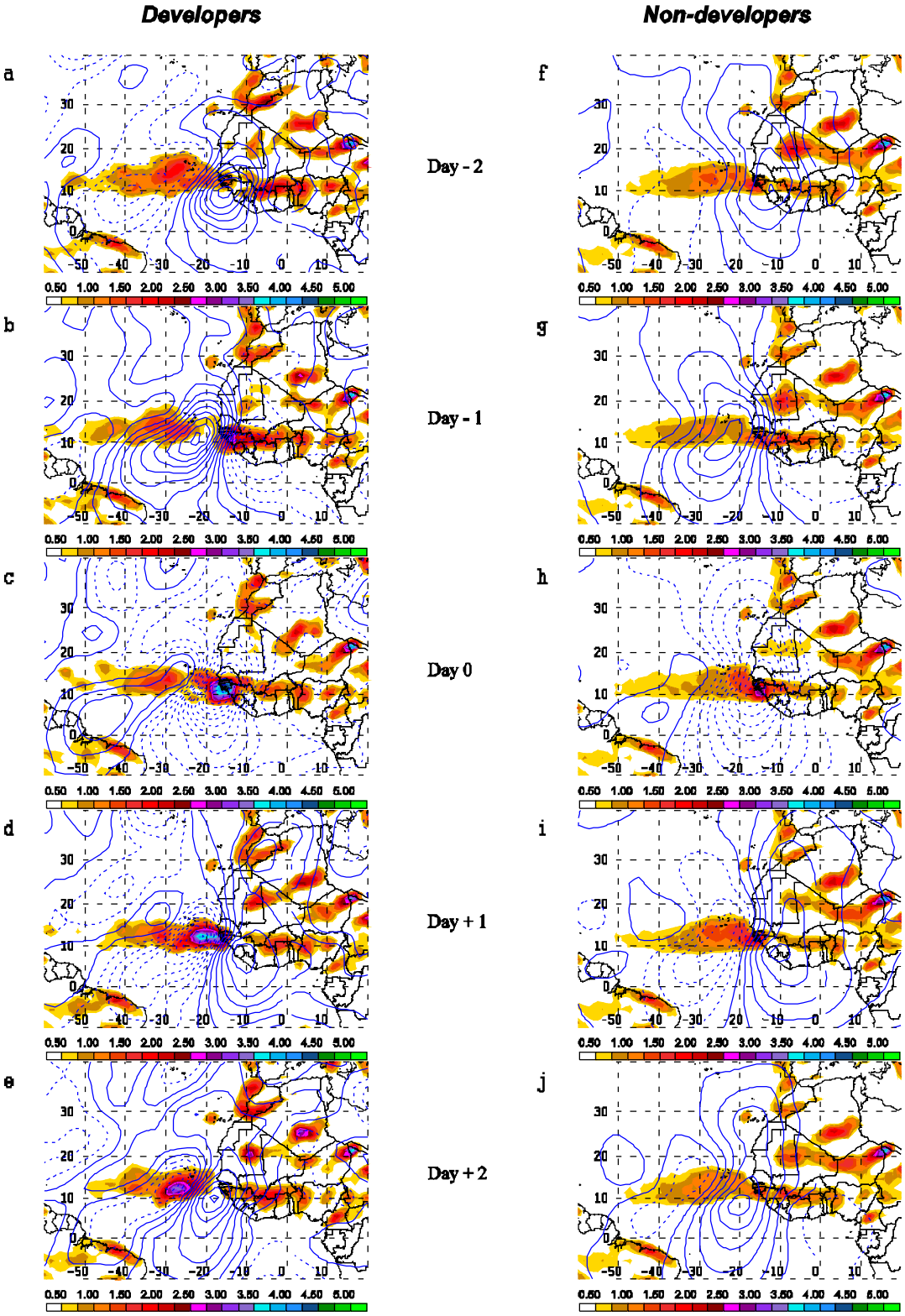

FIG. 3. Composites of developing (left) and non-developing (right) AEWs for the five-day period centered on the day of trough passage at 15°W. Fields shown are 600 hPa streamfunction (solid and dashed lines, based on 2-6 day filtered winds) and 850 hPa relative vorticity (10^{-5} s^{-1}, positive values only, shaded).

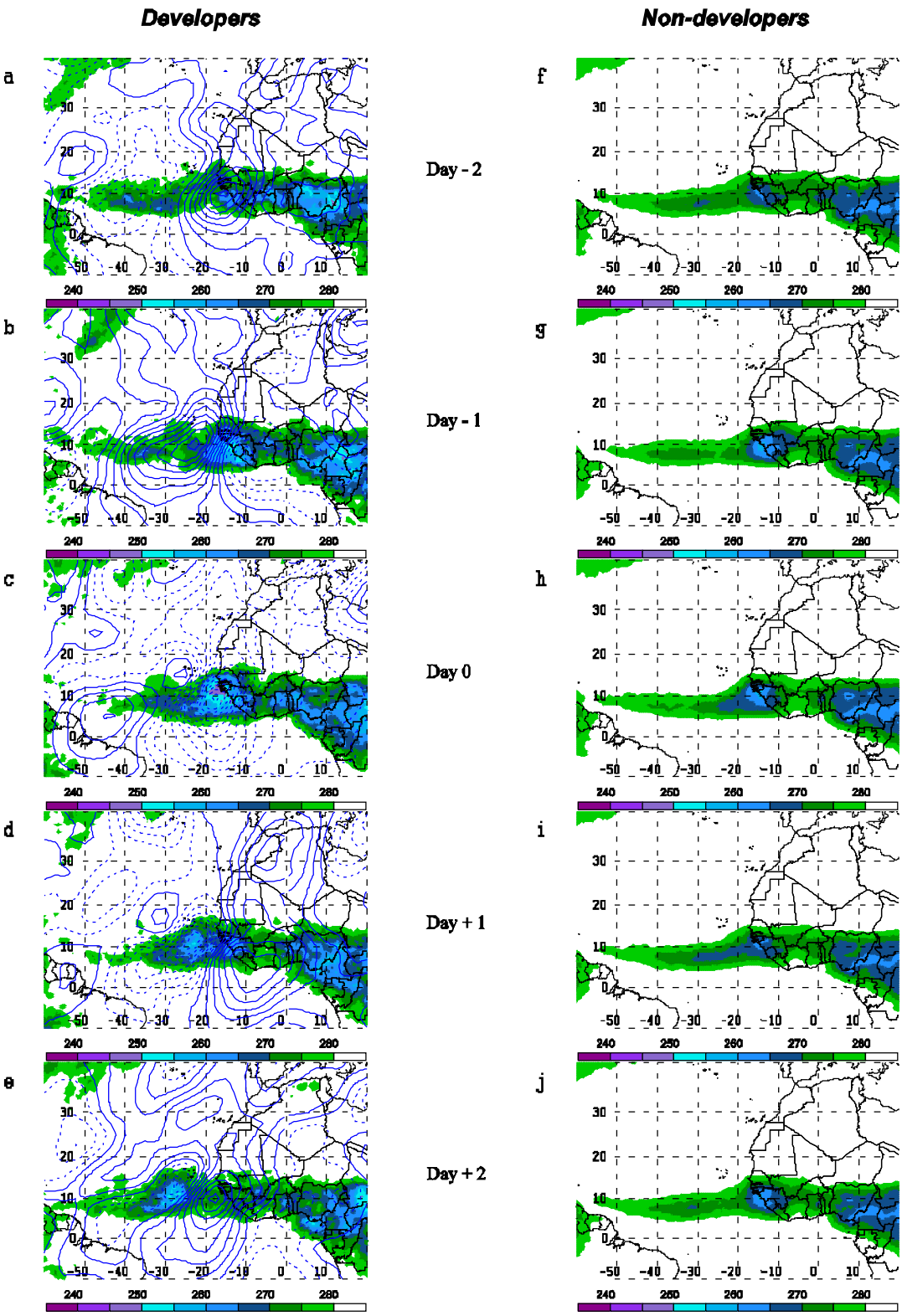

FIG. 4. Composites of developing (left) and non-developing (right) AEWs for the five-day period centered on the day of trough passage at 15°W. Fields shown are 600 hPa streamfunction (solid and dashed lines, based on 2-6 day filtered winds) and brightness temperature (shaded).

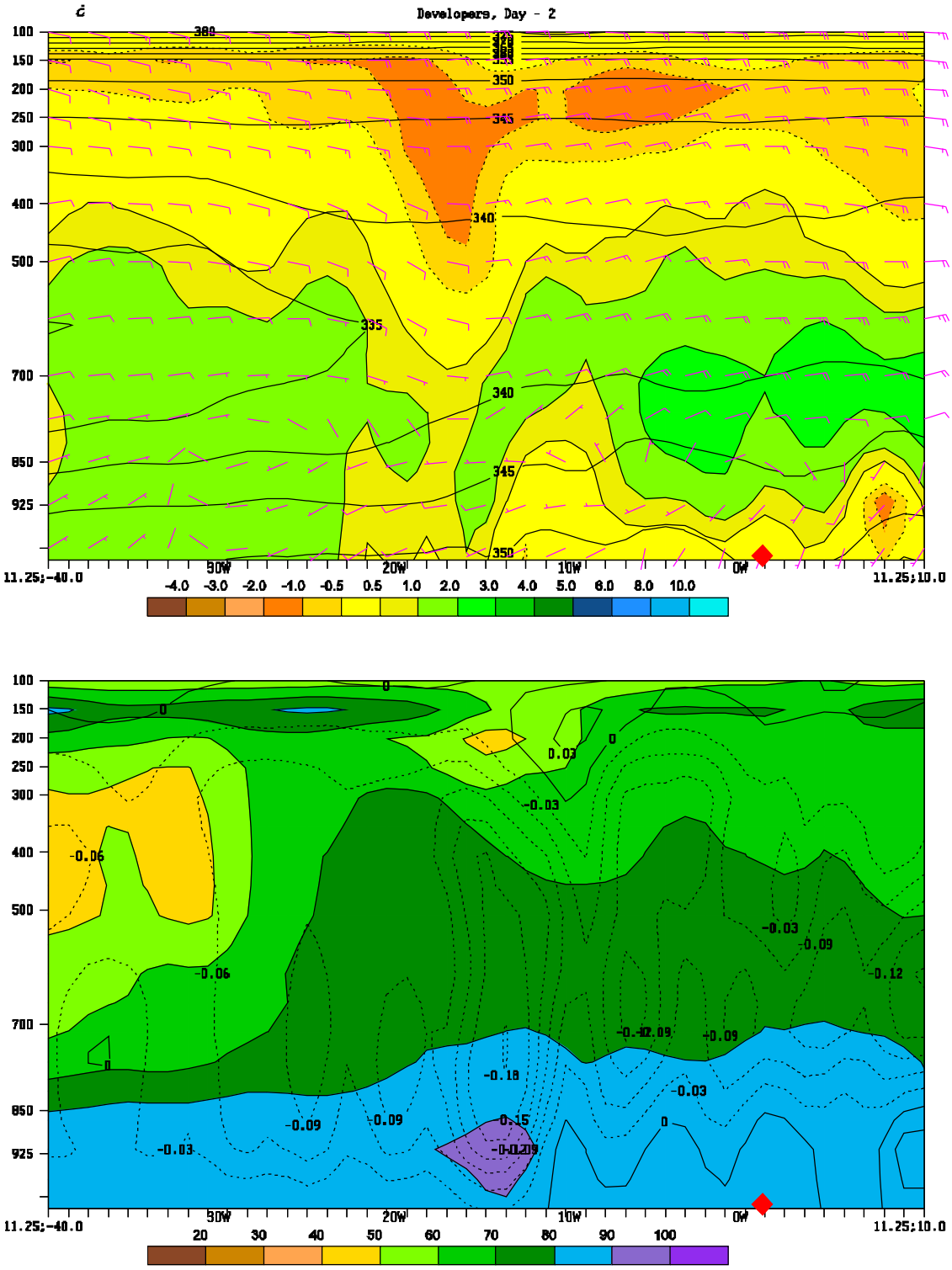

FIG. 5. Cross-sections of the AEW composites for days -2, 0, and +2; developers (non-developers) are displayed in figs. 5a, 5c, and 5e (5b, 5d, 5f). The cross-sections fall along 11.25°N between 40°W and 10°E in the horizontal, and from 1000 hPa to 100 hPa in the vertical. The top half of each figure displays relative vorticity (10^{-5} s^{-1}, shaded), equivalent potential temperature (degrees K, black contours), and horizontal wind barbs (knots). The bottom half shows relative humidity (%, shaded) and vertical velocity (hPa s^{-1}, black contours). The approximate location of the composite AEW trough is indicated by the red diamond.

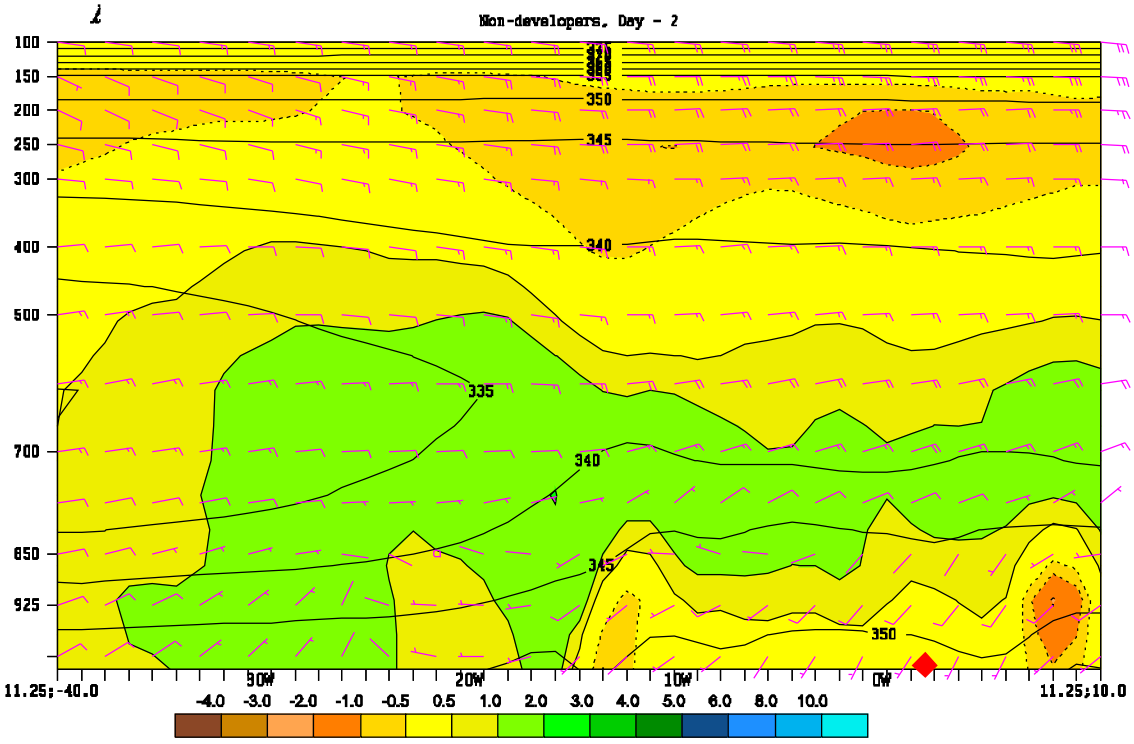
Non-developers, Day - 2
100
150
200
250
300
400
500
700
850
925
350
345
340
335
340
345
350
30W
20W
10W
0W
11.25;-40.0
11.25;10.0
-4.0 -3.0 -2.0 -1.0 -0.5 0.5 1.0 2.0 3.0 4.0 5.0 6.0 8.0 10.0

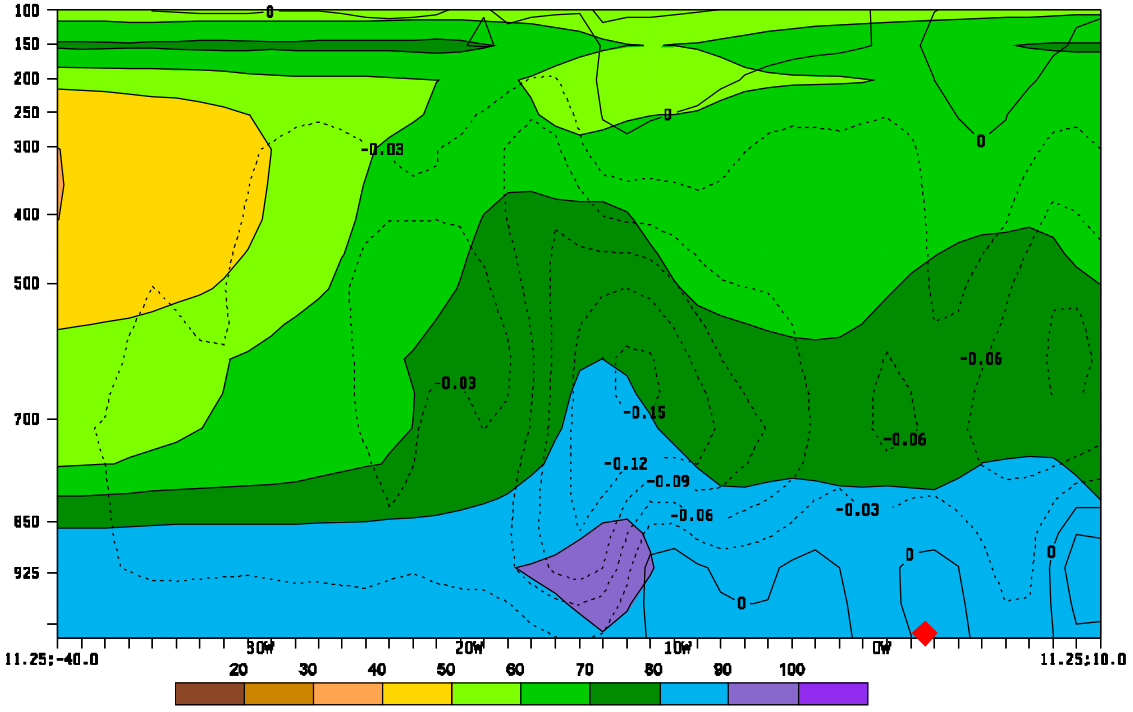
100
150
200
250
300
400
500
700
850
925
0
-0.03
-0.03
-0.06
-0.06
-0.15
-0.12
-0.09
-0.06
-0.03
30W
20W
10W
0W
11.25;-40.0
11.25;10.0
20 30 40 50 60 70 80 90 100

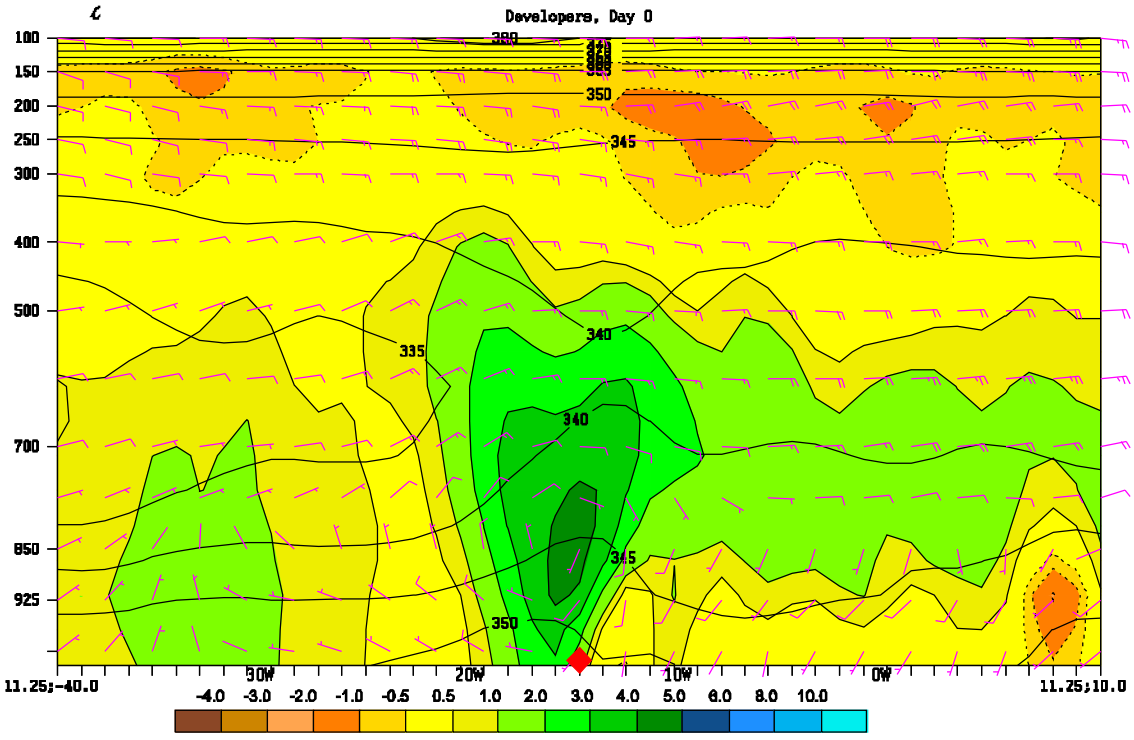
Developers, Day 0
100
150
200
250
300
400
500
700
850
925
350
345
340
335
11.25;-40.0
30W
20W
10W
0W
11.25;10.0
-4.0 -3.0 -2.0 -1.0 -0.5 0.5 1.0 2.0 3.0 4.0 5.0 6.0 8.0 10.0

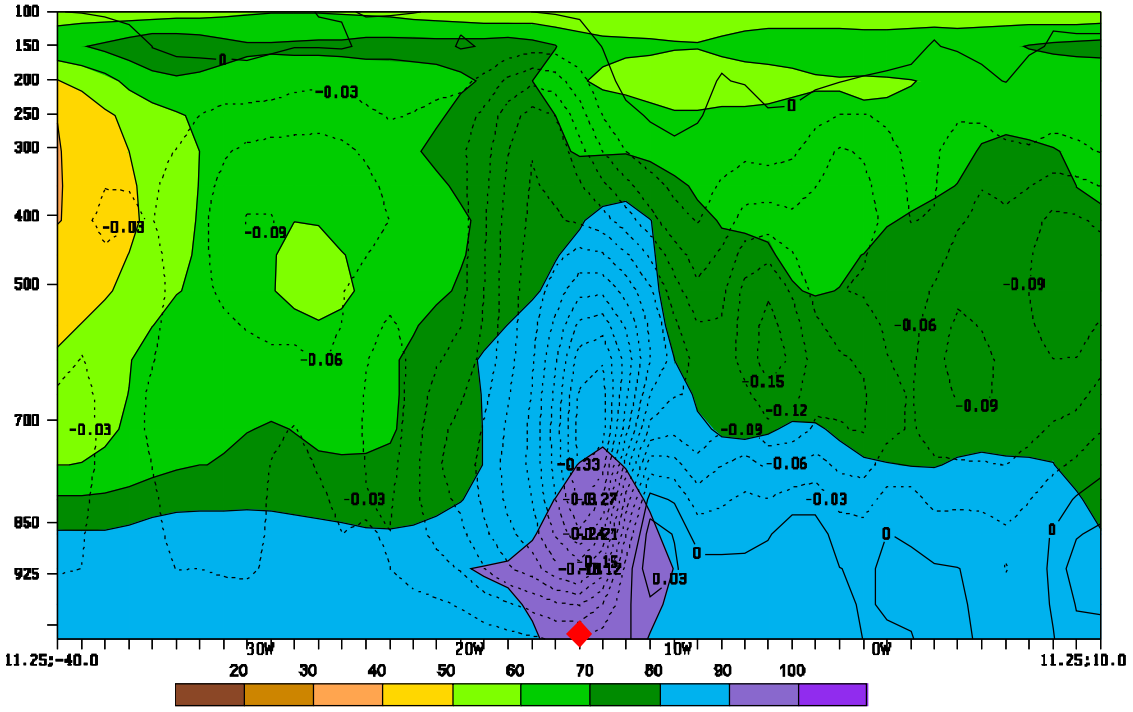
100
150
200
250
300
400
500
700
850
925
0
-0.03
-0.09
-0.06
-0.15
-0.12
-0.33
-0.27
-0.21
-0.18
11.25;-40.0
30W
20W
10W
0W
11.25;10.0
20 30 40 50 60 70 80 90 100

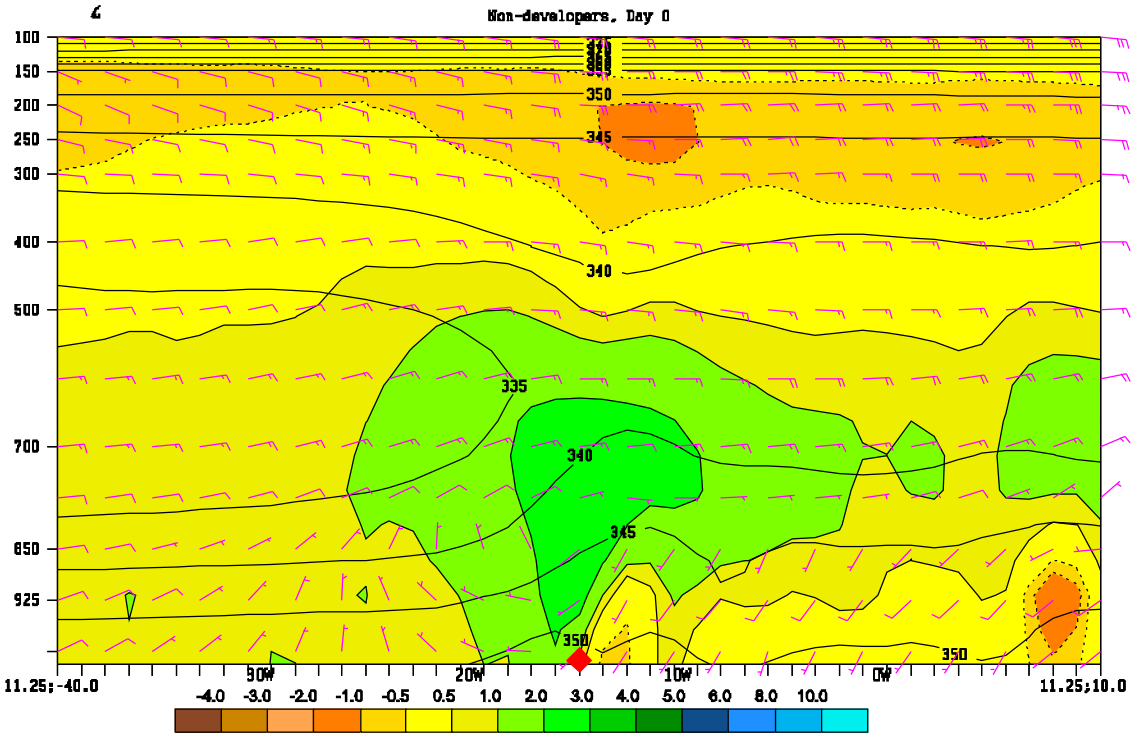
Non-developers, Day 0
100
150
200
250
300
400
500
700
850
925
350
345
340
335
340
345
350
350
30W
20W
10W
0W
11.25,-40.0
11.25,10.0
-4.0 -3.0 -2.0 -1.0 -0.5 0.5 1.0 2.0 3.0 4.0 5.0 6.0 8.0 10.0

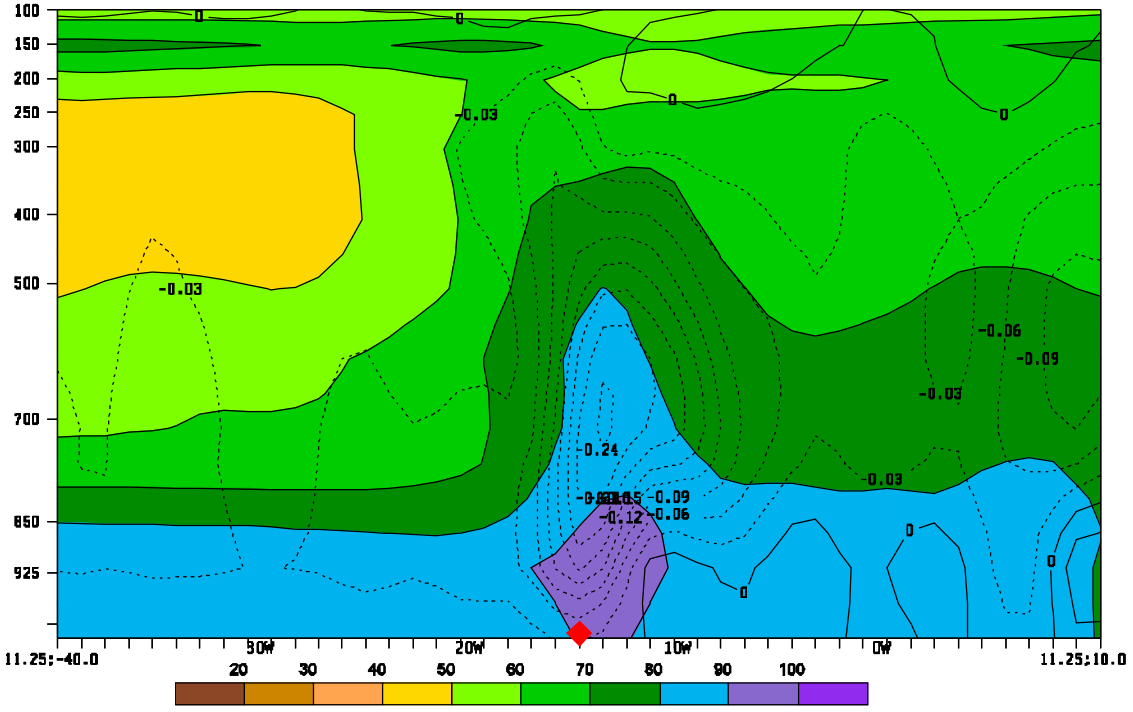
100
150
200
250
300
400
500
700
850
925
0
0
-0.03
0
0
-0.03
-0.06
-0.09
-0.03
0.24
-0.03
-0.09
-0.06
0
0
0
30W
20W
10W
0W
11.25,-40.0
11.25,10.0
20 30 40 50 60 70 80 90 100

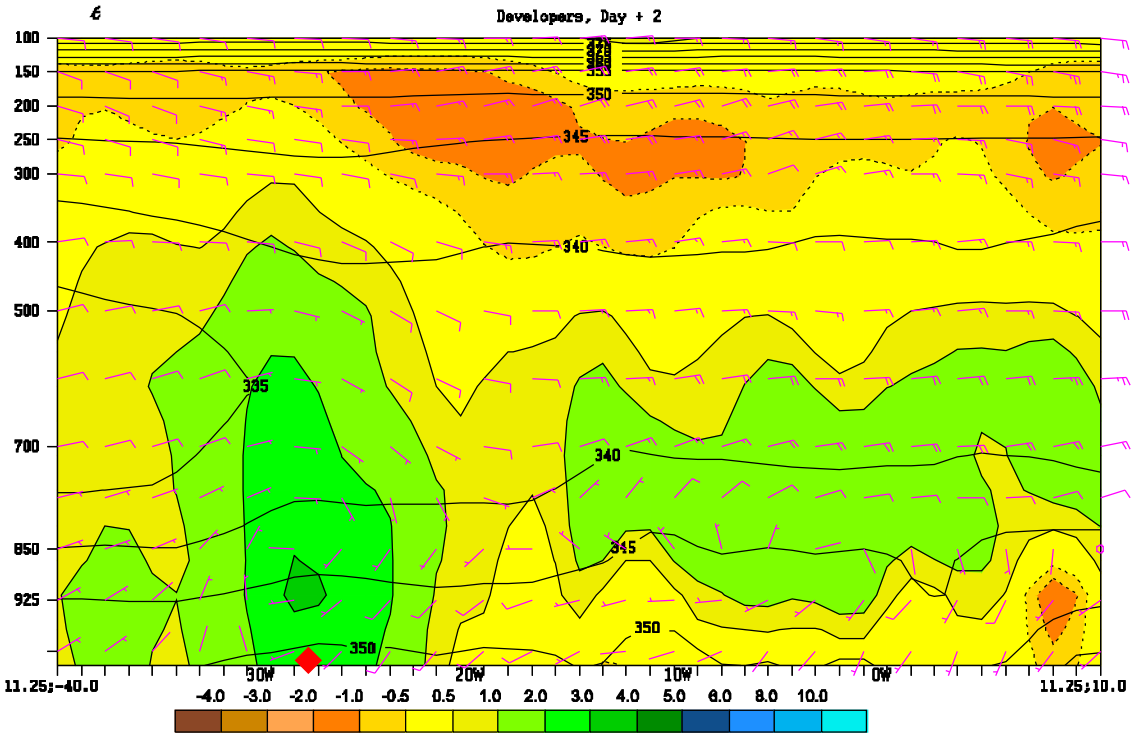
Developers, Day + 2
100
150
200
250
300
400
500
700
850
925
350
345
340
335
11.25;-40.0
30W
20W
10W
0W
11.25;10.0
-4.0 -3.0 -2.0 -1.0 -0.5 0.5 1.0 2.0 3.0 4.0 5.0 6.0 8.0 10.0

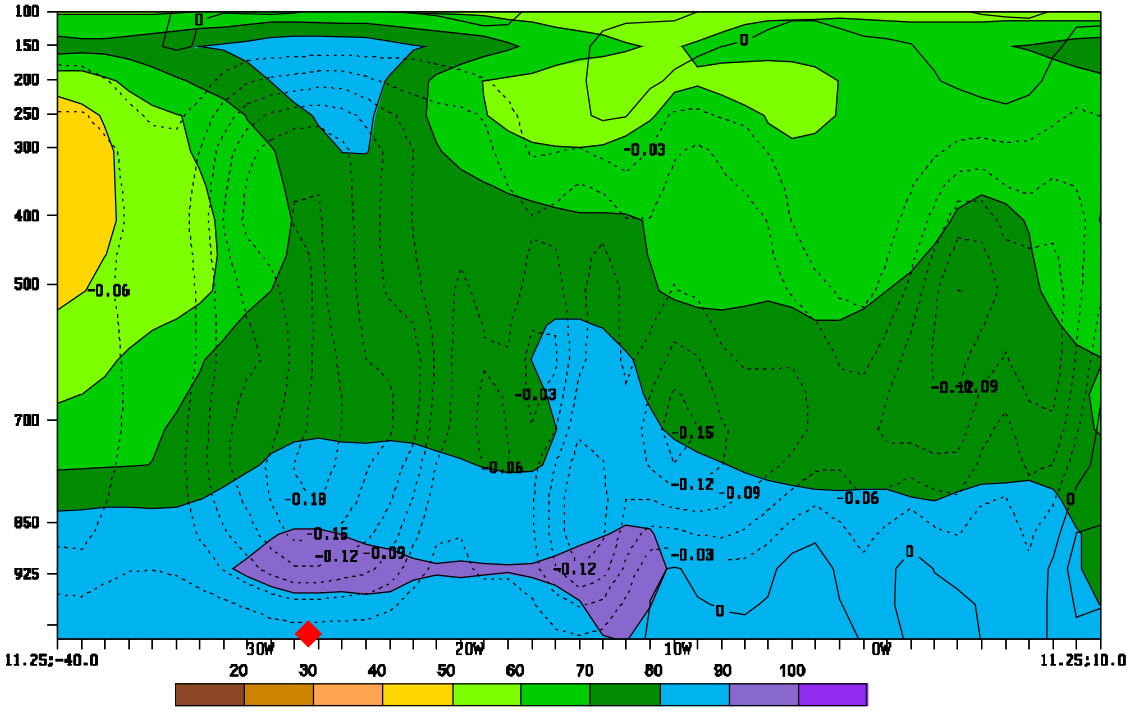
100
150
200
250
300
400
500
700
850
925
0
-0.03
-0.06
-0.09
-0.12
-0.15
-0.18
11.25;-40.0
30W
20W
10W
0W
11.25;10.0
20 30 40 50 60 70 80 90 100

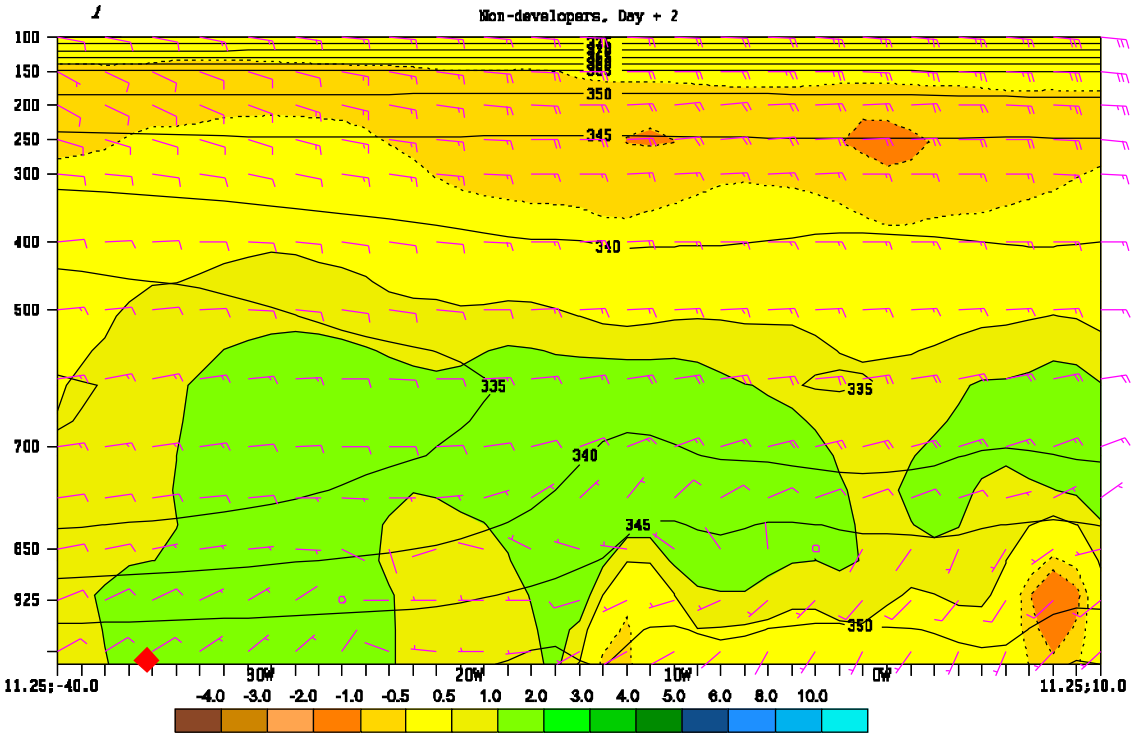
1
Non-developers, Day + 2
100
150
200
250
300
400
500
700
850
925
350
345
340
335
335
340
345
350
11.25;-40.0
30W
20W
10W
0W
11.25;10.0
-4.0 -3.0 -2.0 -1.0 -0.5 0.5 1.0 2.0 3.0 4.0 5.0 6.0 8.0 10.0

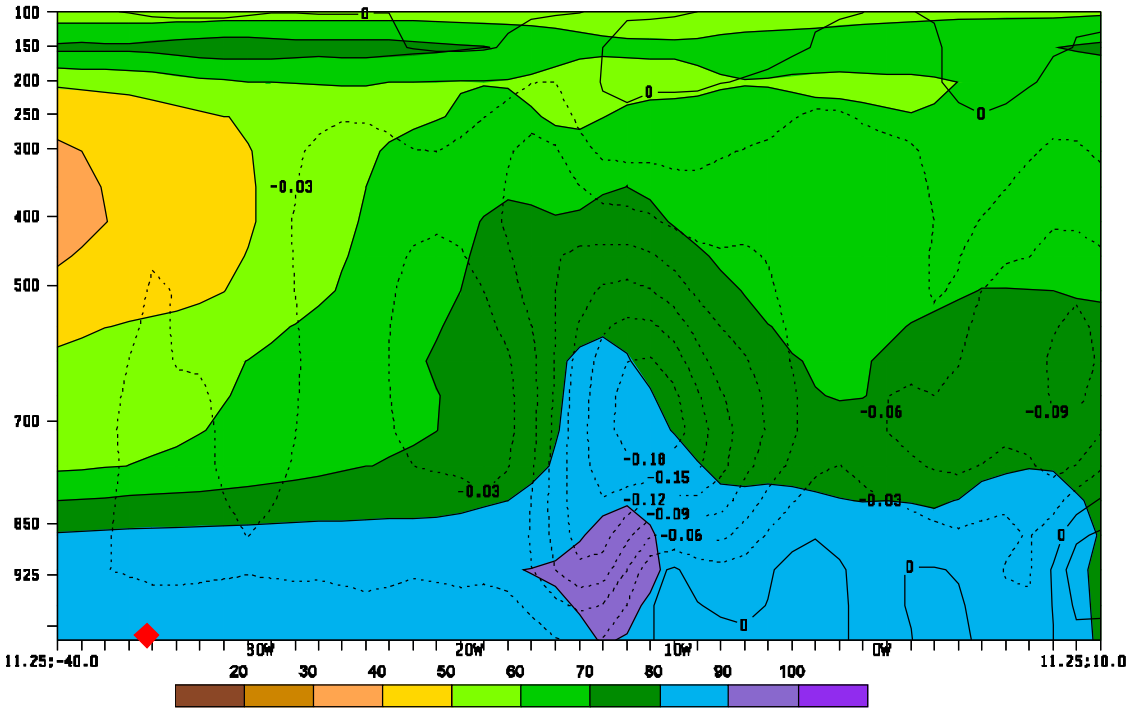
100
150
200
250
300
400
500
700
850
925
0
0
0
-0.03
-0.03
-0.06
-0.09
-0.10
-0.15
-0.12
-0.09
-0.06
-0.03
0
0
0
11.25;-40.0
30W
20W
10W
0W
11.25;10.0
20 30 40 50 60 70 80 90 100

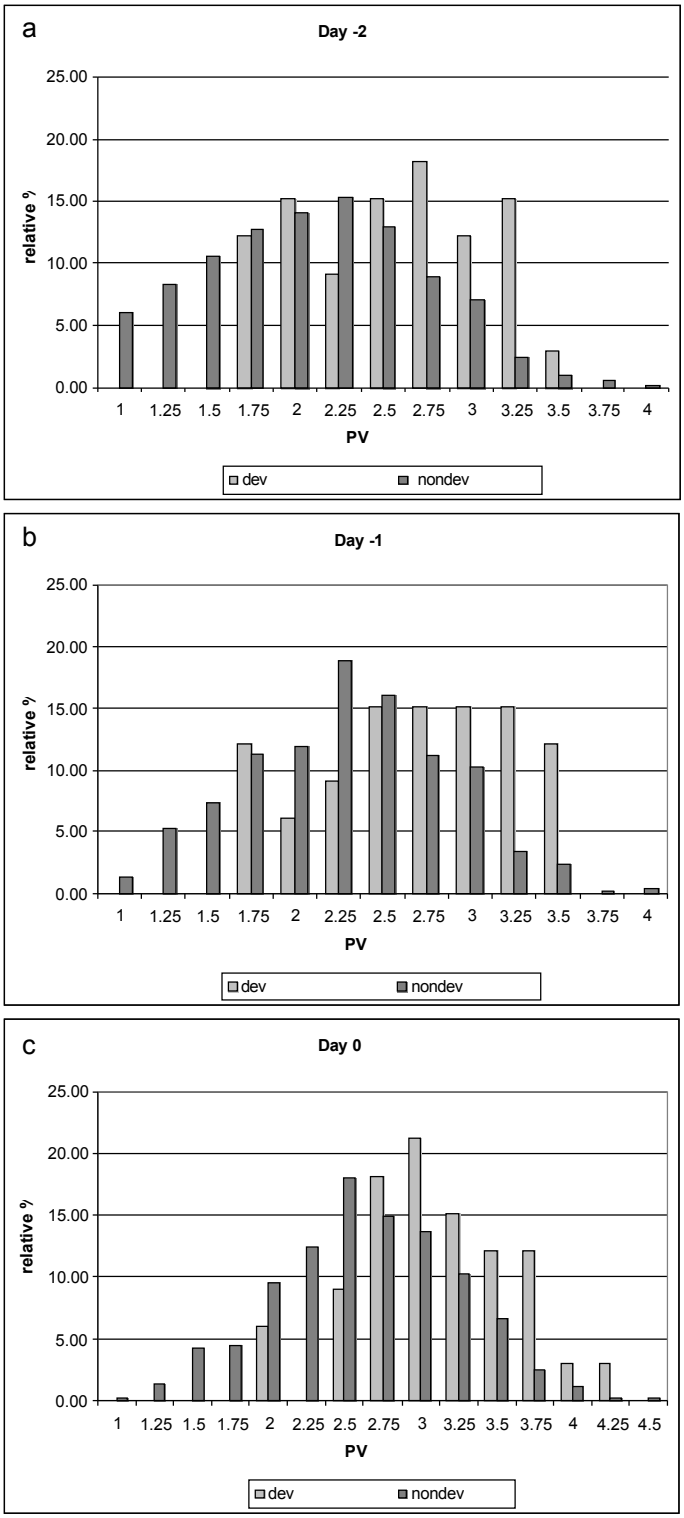

FIG. 6. histograms of PV (PVU) at 600hPa for the developing (light gray bars) and non-developing AEWs (dark gray bars) for (a) day -2 (b) day -1 and (c) day 0. The sampled trough locations for the three days covered an 8°x10° lat-lon box with bounds 8°-16°N (all three days), 5°W-5°E for day -2, 15°W-5°W for day -1 and 20°W-10°W for day 0.

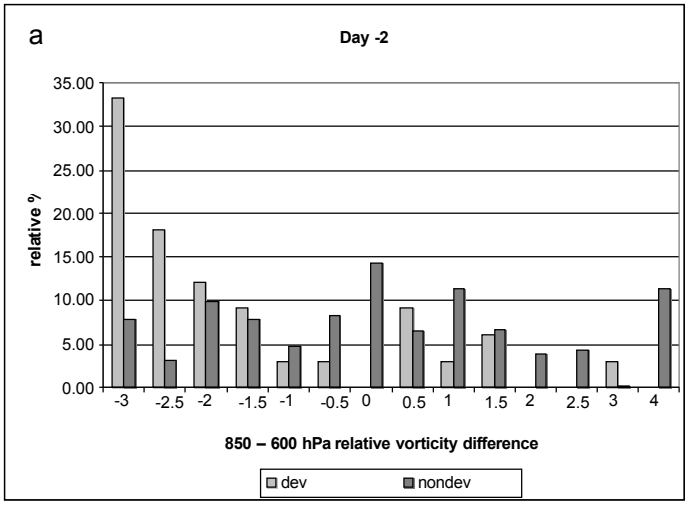

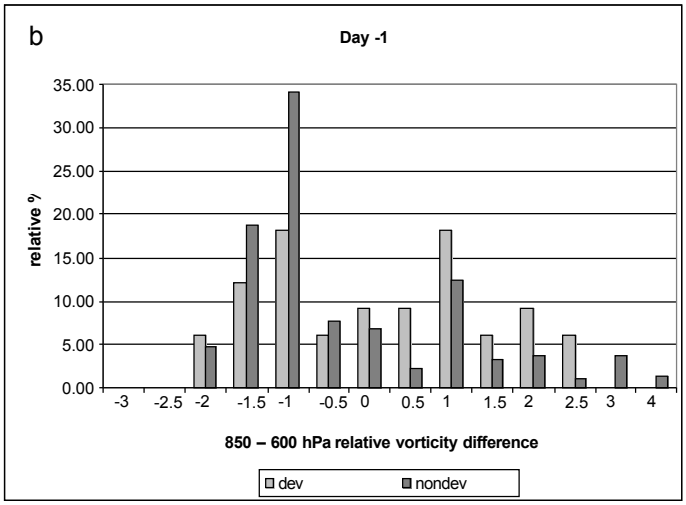

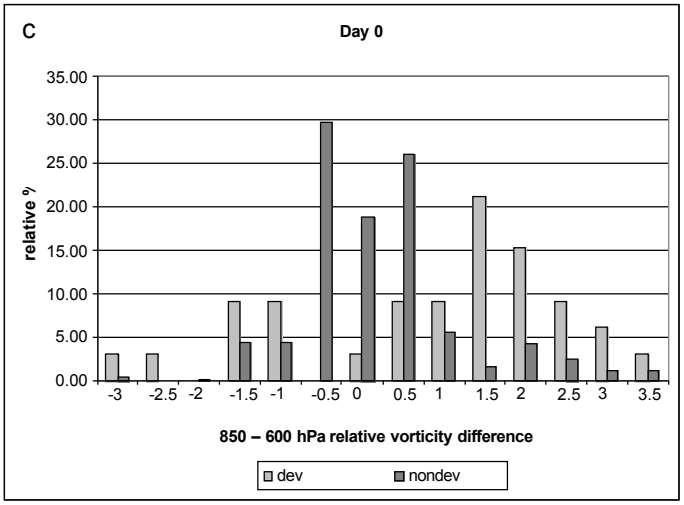

FIG. 7. As in FIG. 6. but for the difference in relative vorticity (10^{-5} s^{-1}) between 850 and 600 hPa for (a) day -2, (b) day -1 and (c) day 0. Positive (negative) values of the difference denote greater (less) vorticity at 850 hPa than at 600 hPa.

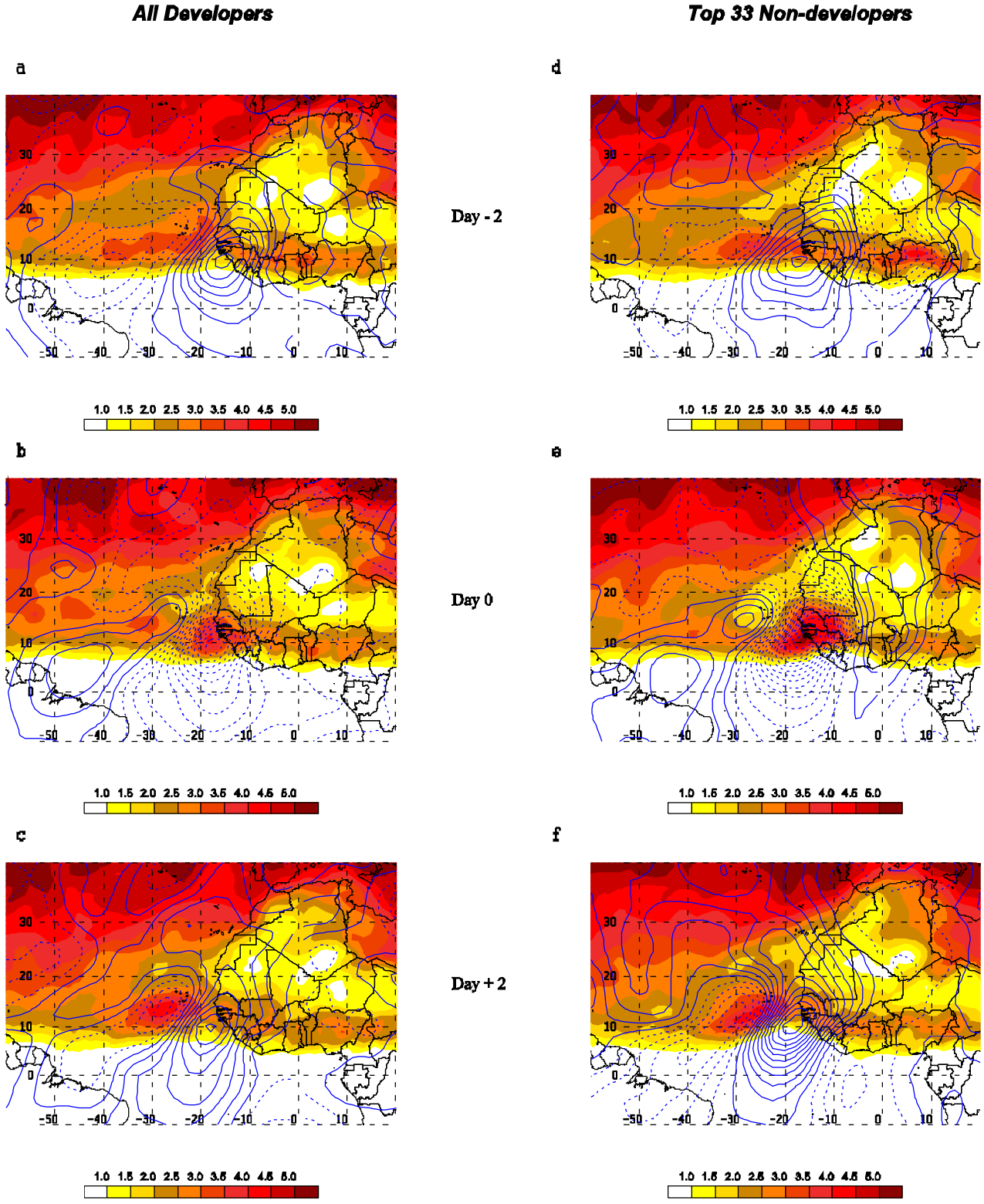

FIG. 8. Composites of developing (left) and the 33 most intense non-developing (right) AEWs for days -2, 0, and +2. Fields shown are 600 hPa streamfunction (solid and dashed lines, based on 2-6 day filtered winds) and 600 hPa potential vorticity (shaded).

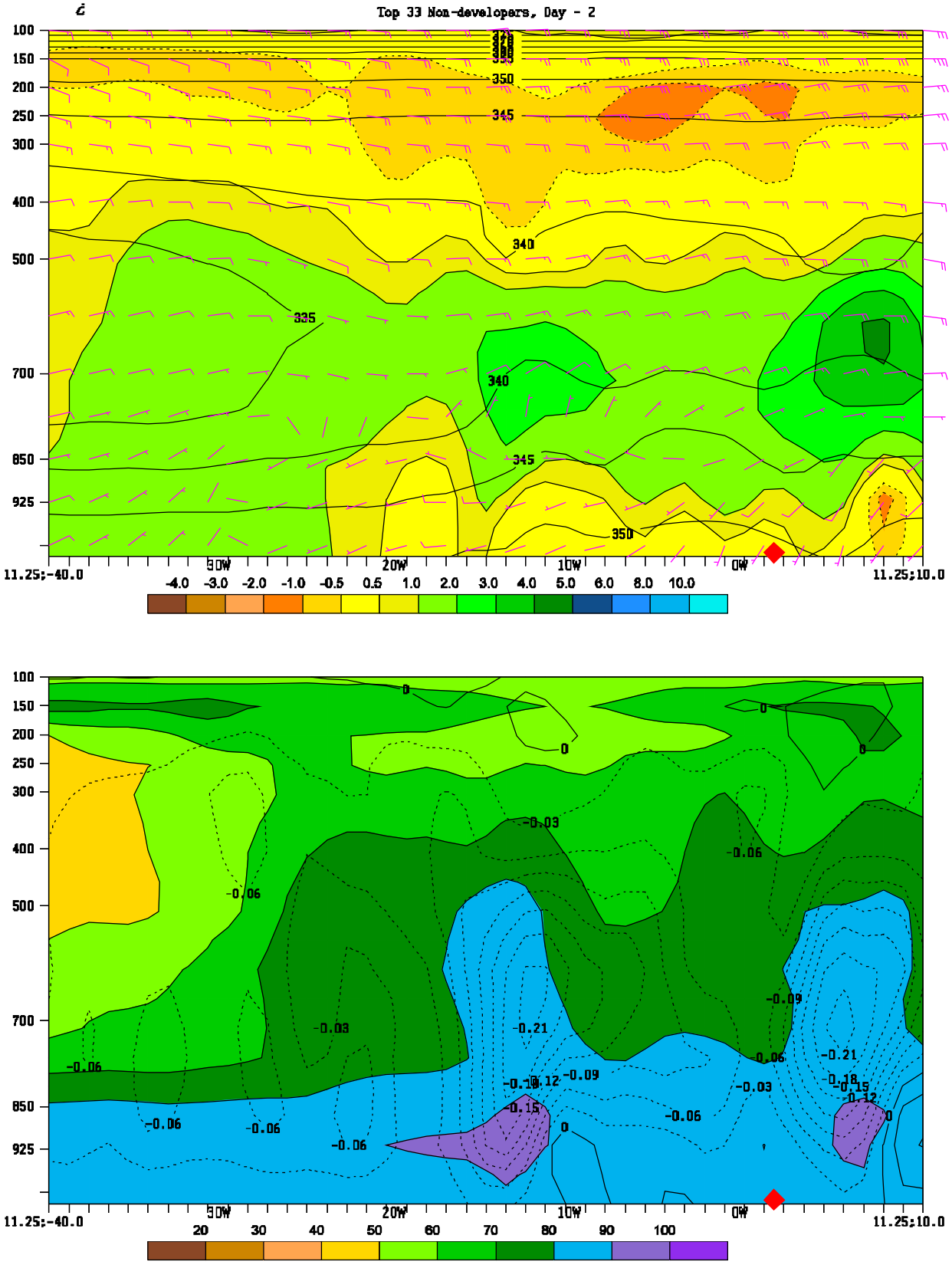

FIG. 9. As in Fig. 5 a-c, but for the 33 most intense non-developing AEWs.

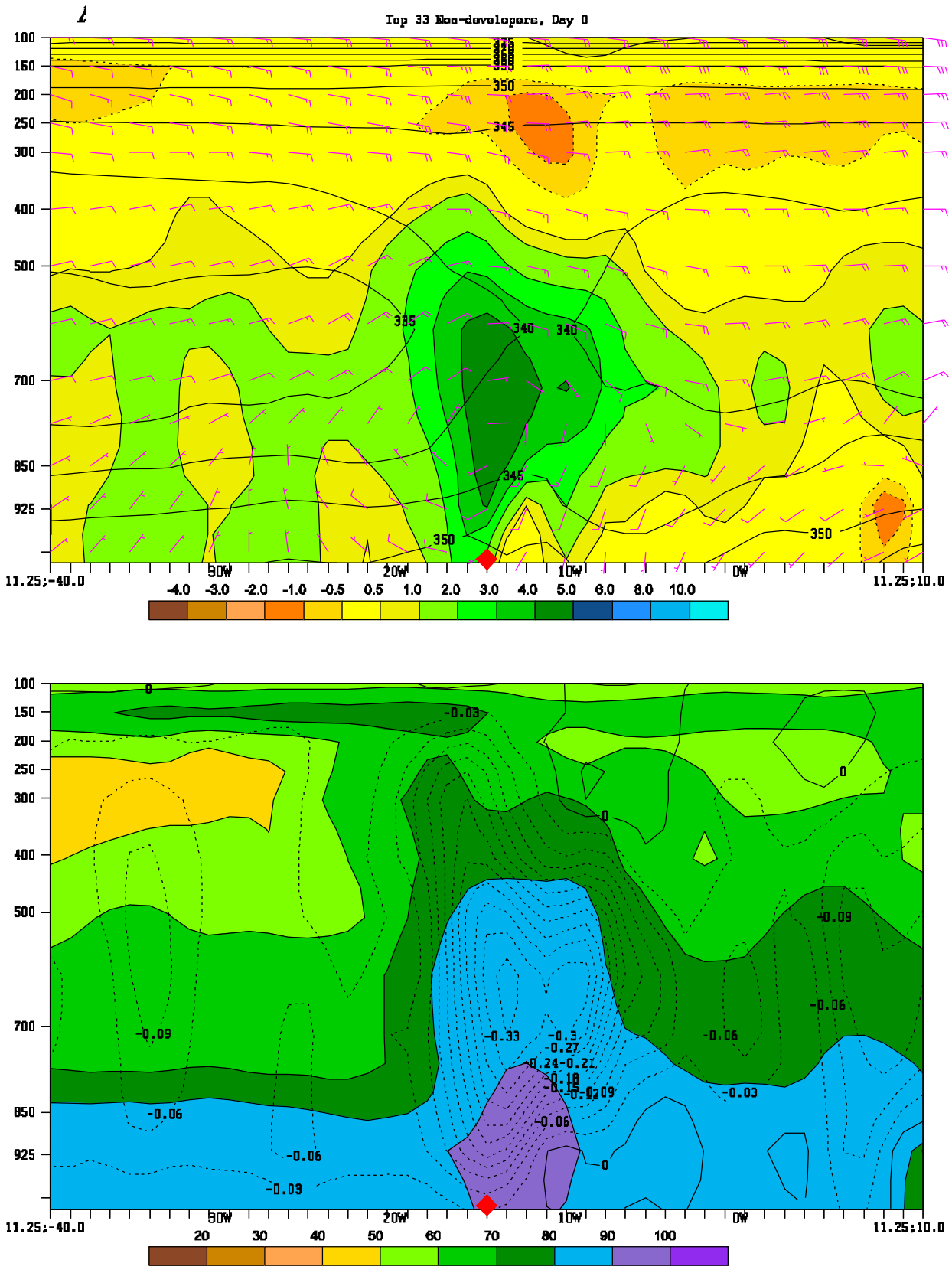
Top 33 Non-developers, Day 0
100
150
200
250
300
400
500
700
850
925
350
345
335
340
340
345
350
350
11.25;-40.0
30W
20W
10W
0W
11.25;10.0
-4.0 -3.0 -2.0 -1.0 -0.5 0.5 1.0 2.0 3.0 4.0 5.0 6.0 8.0 10.0
0
-0.03
0
0
-0.09
-0.06
-0.09
-0.33
-0.3
-0.27
-0.24
-0.21
-0.18
-0.15
-0.12
-0.09
-0.06
-0.06
-0.03
-0.06
-0.06
-0.03
0
20 30 40 50 60 70 80 90 100

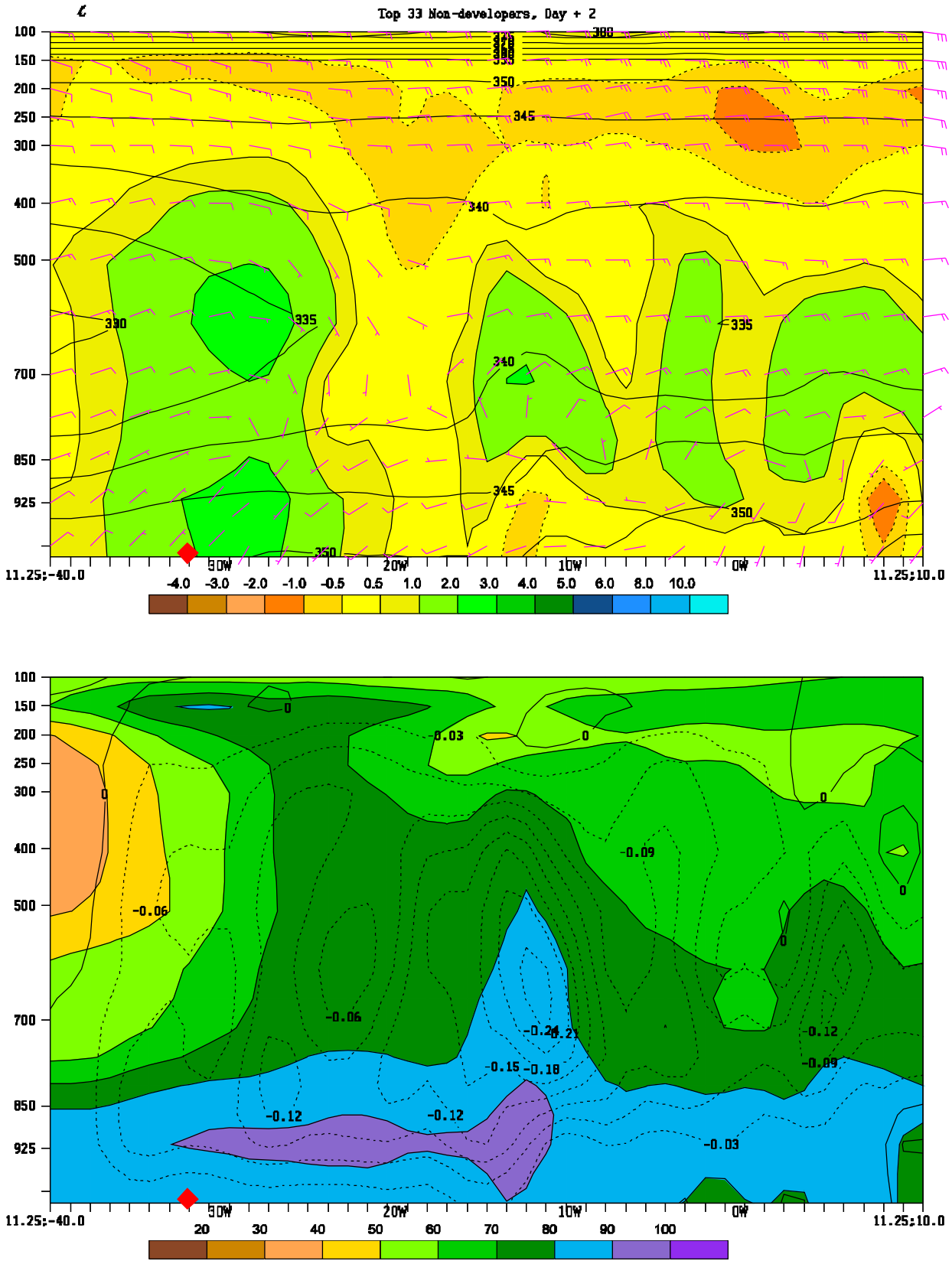
Top 33 Non-developers, Day + 2
100
150
200
250
300
400
500
700
850
925
380
350
345
340
335
330
350
345
340
335
350
11.25:-40.0
50W
20W
10W
0W
11.25:10.0
-4.0 -3.0 -2.0 -1.0 -0.5 0.5 1.0 2.0 3.0 4.0 5.0 6.0 8.0 10.0
0
-0.03
0
0
0
-0.09
0
-0.06
0
-0.06
-0.24
-0.21
-0.12
-0.15
-0.18
-0.09
-0.12
-0.12
-0.03
20 30 40 50 60 70 80 90 100

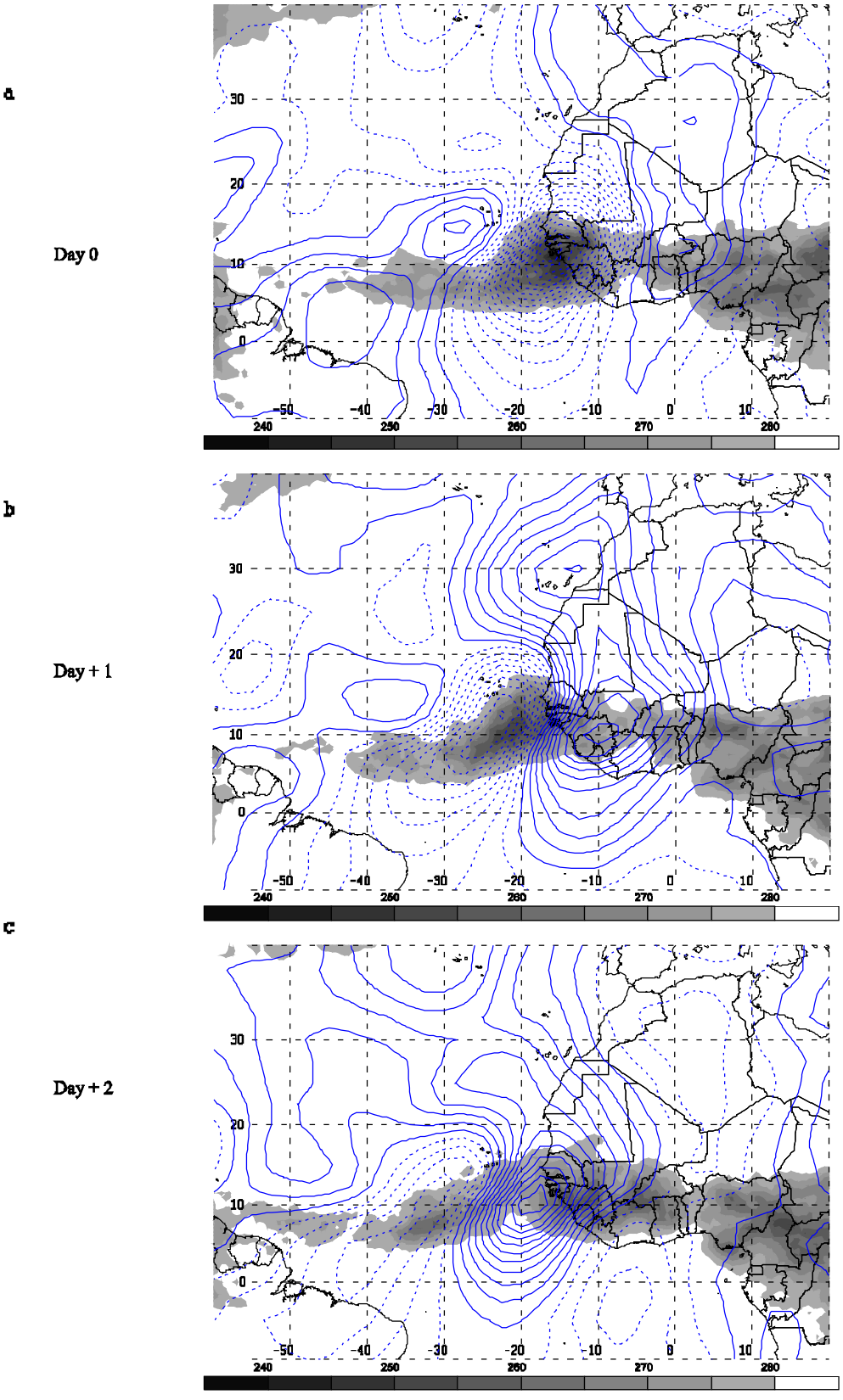

FIG. 10. 600 hPa streamfunction (contour lines) and CLAUS brightness temperature for the 33 most intense non-developing AEWs.

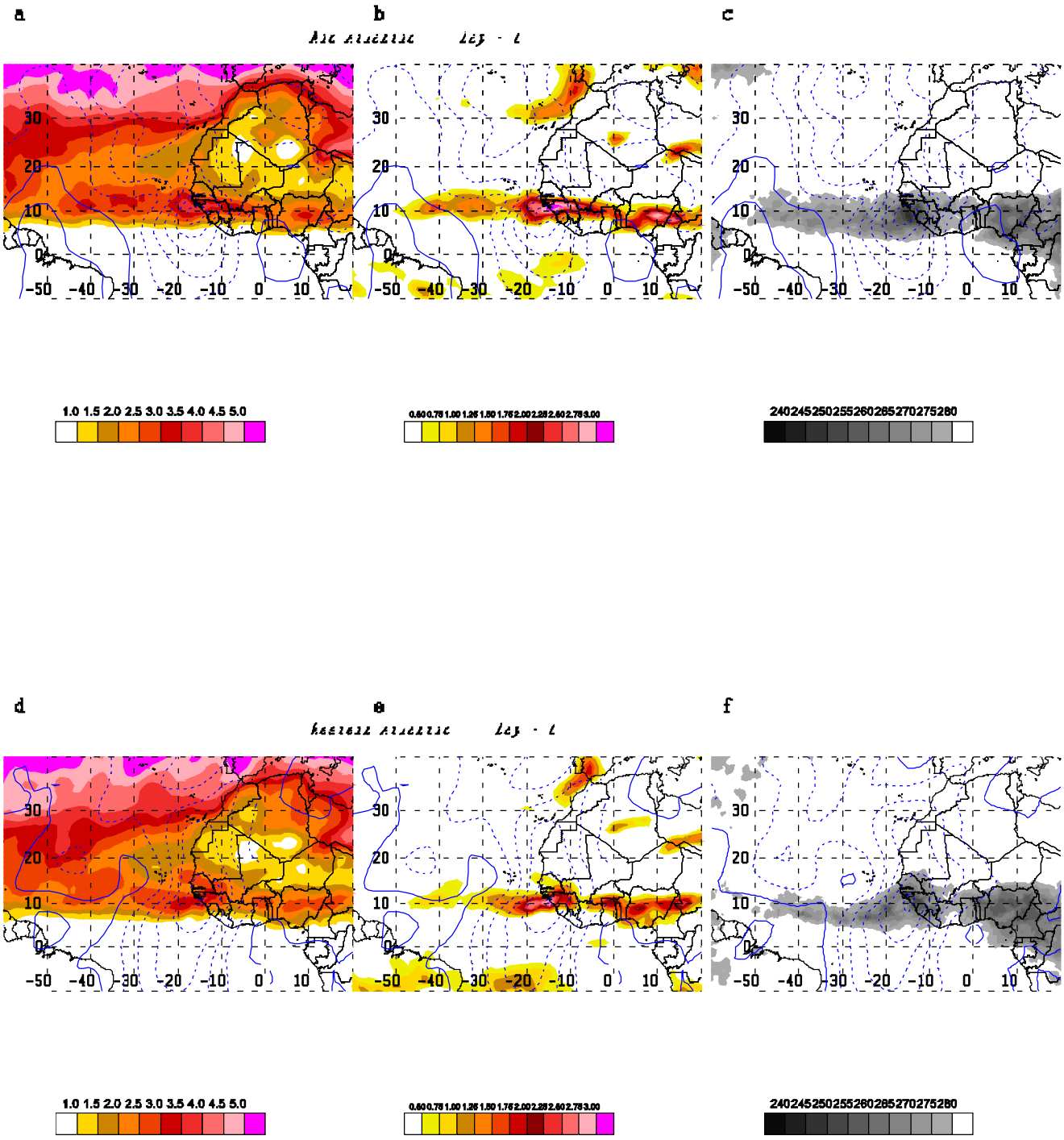

FIG. 11. Day 0 600 hPa streamfunction, overlaid with (a) 600 hPa potential vorticity (PVU, shaded); (b) 600 hPa relative vorticity ($10^{-5}s^{-1}$, shaded); (c) CLAUS brightness temperature (K, shaded) for developers in the mid-Atlantic region of the MDR; (d-f) are as in (a-c), but for the western Atlantic.

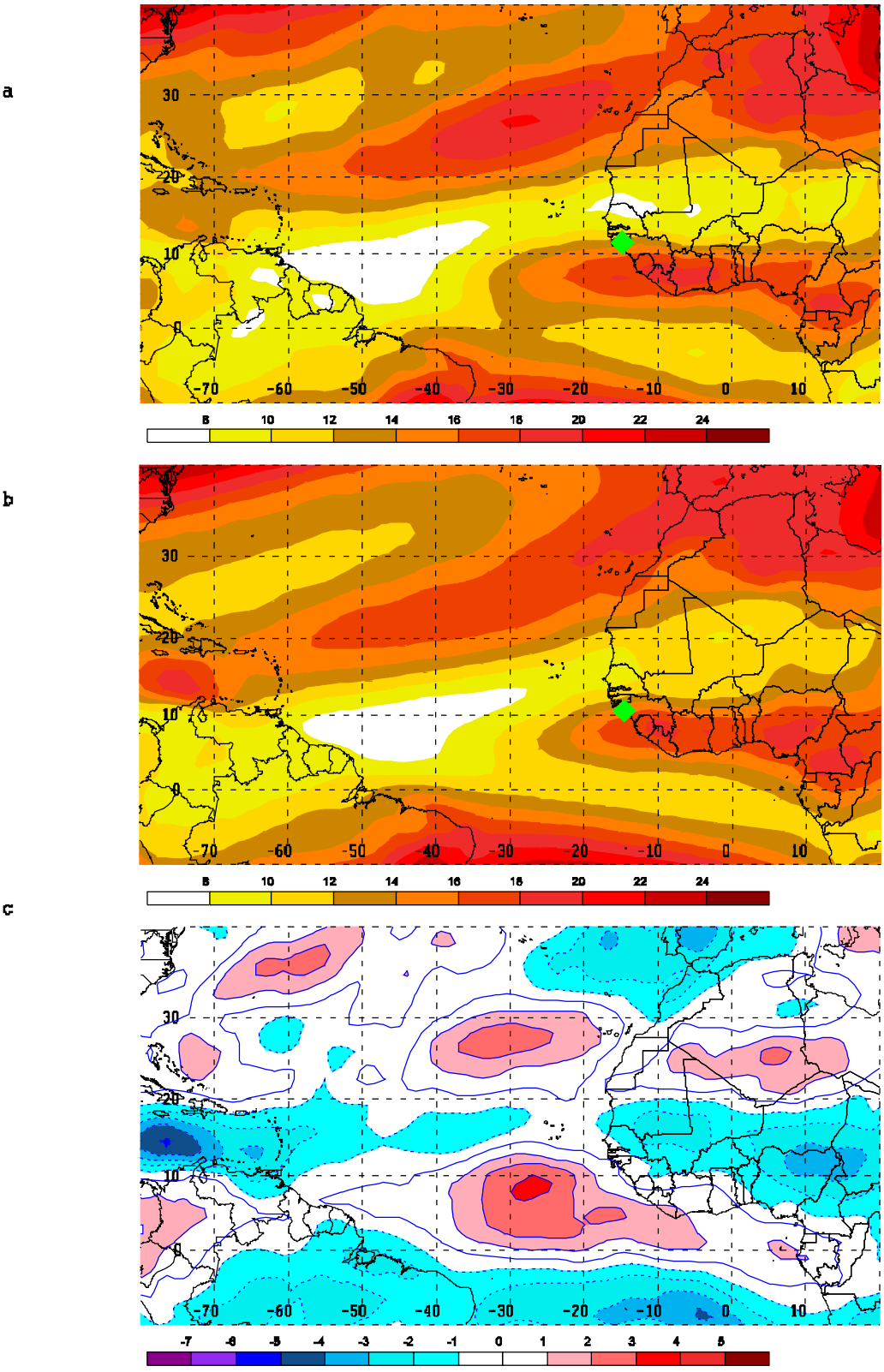

FIG. 12. Day -2 to day +2 average of composite wind shear (m s^{-1}) between 200 and 850 hPa of (a) developing and (b) non-developing AEWs and (c) the difference between (a) and (b). The position of the composite 850 hPa relative vorticity maximum is shown by the green diamond in (a) and (b).

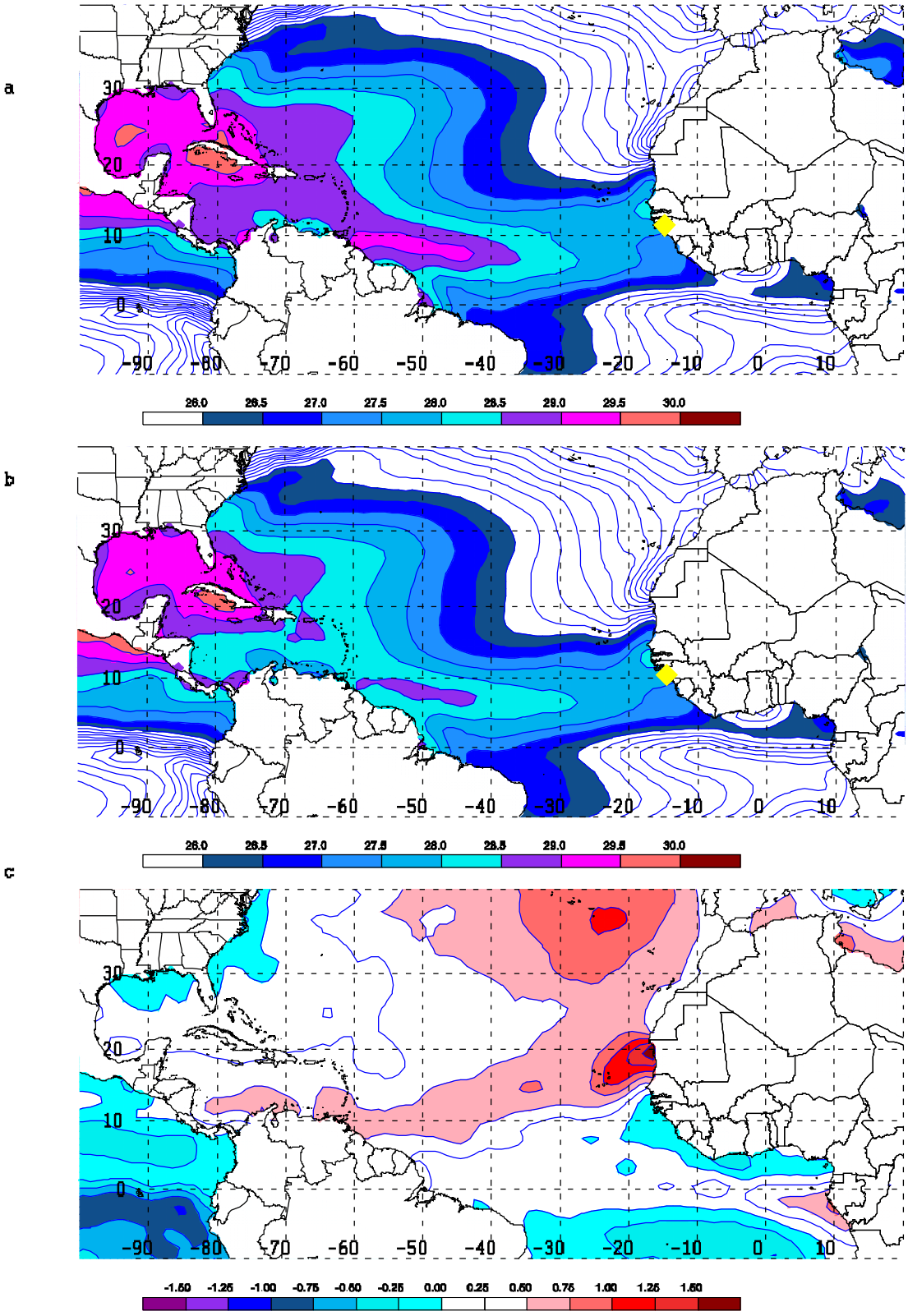

FIG. 13. Composite of weekly SST (K) for (a) developers and (b) non-developers, with (c) the difference between (a) and (b). The position of the composite 850 hPa relative vorticity maximum is shown by the yellow diamond in (a) and (b).

Number	July	August	September	JAS-Total
Developing	12	44	35	91
Non-Developing	188	164	160	512
East Atlantic Developing	3	13	17	33
Mid-Atlantic Developing	5	19	6	30
West Atlantic Developing	4	12	12	28

Table 1: Number of developing and non-developing AEWs per month (top two rows); and the number of named tropical cyclones associated with AEWS according to where they were first named (bottom three rows). East Atlantic is represented by the box between 7^{o}N-20^{o}N and 30^{o}W-15^{o}W. Mid-Atlantic is represented by the box between 7^{o}N-20^{o}N and 45^{o}W-30^{o}W. West Atlantic is represented by the box between 7^{o}N-20^{o}N and 60^{o}W-45^{o}W.